5-2019

Feasibility Study of a Novel Ground Heat Exchanger using Phase-Change Materials

Joseph Keith Warner
University of Tennessee, jwarner7@vols.utk.edu

To the Graduate Council:

I am submitting herewith a thesis written by Joseph Keith Warner entitled "Feasibility Study of a Novel Ground Heat Exchanger using Phase-Change Materials." I have examined the final electronic copy of this thesis for form and content and recommend that it be accepted in partial fulfillment of the requirements for the degree of Master of Science, with a major in Mechanical Engineering.

Zhili Zhang, Major Professor

We have read this thesis and recommend its acceptance:

Xiaibing Liu

Accepted for the Council:
Dixie L. Thompson

Vice Provost and Dean of the Graduate School

(Original signatures are on file with official student records.)

Feasibility Study of a Novel Ground Heat Exchanger using Phase-Change Materials

A Thesis Presented for the
Master of Science
Degree
The University of Tennessee, Knoxville

Joseph Keith Warner
May 2019

ACKNOWLEDGEMENTS

I would like to thank Dr. Xiaobing Liu for his support, guidance, and collaboration during my tenure in graduate school. His willingness to teach and mentor me over the years has greatly impacted my life, and I am deeply grateful.

I would also like to thank Dr. Zhili Zhang for his guidance during my tenure at the University of Tennessee. If not for his trust I would not be in this position today. His advice and guidance has been invaluable over the years, and is greatly appreciated.

Special thanks to Dr. Hans DeSmidt for his help and guidance as a committee member for the preparation and defense of my thesis.

I would also like to thank Dr. Mingkan Zhang, Dr. Kaushik Biswas, Dr. Ming Qu, and Liang Shi for their collaboration during this project. This thesis would not have been possible without their contributions.

ABSTRACT

The performance of a novel ground heat exchanger, the Underground Thermal Battery (UTB), was investigated in this paper. The UTB is an alternative to the conventional ground heat exchanger (GHE) which is designed to be installed in the shallow subsurface of the ground (less than 20 ft. deep). This can reduce the cost of drilling associated with the installation of boreholes in the conventional vertical bore ground heat exchanger (VBGHE). The UTB is a tank, 2-3 ft. in diameter, which is filled with water. The tank has a large thermal capacity which reduces the temperature response of the tank for a given thermal load. PCM is suspended in the tank water to further increase the thermal capacity. A simplified 1-D model has been developed to simulate the UTB over a year of operation. This model was validated against a 3-D CFD model. The performance of the UTB is compared with the conventional VBGHE under various operating conditions. The results indicate that a UTB with two tanks can offer similar performance as the VBGHE under most conditions. Simulation results indicate that, by integrating with UTB with the lawn irrigation system of a residence, the performance of the UTB is improved and thereby the size needed to meet the thermal demands can be reduced without any additional water consumption. A preliminary cost analysis suggests that the UTB may offer significant cost savings potential over the conventional VBGHE.

TABLE OF CONTENTS

LIST OF TABLES

LIST OF FIGURES

LIST OF SYMBOLS

Symbol	Description	Units
T	Temperature	C
c_p	Heat capacity	J/kg·K
ρ	Density	kg/m^3
q_{soil}	Heat transfer to soil	J
q_{HEX}	Heat transfer from heat exchanger	J
q_{PCM}	Heat transfer to PCM	J
V_{tank}	volume of UTB tank	m^3
$\vec{r}_s$	Soil node vector	-
P	Logarithmic power of soil node distribution	-
$\vec{u}$	Base vector for soil nodes	-
n_s	Number of soil nodes	-
r	Radial coordinate	m
Δr	Special increment	m
Δr_{min}	Minimum special increment for stability	m
α	Thermal diffusivity	m^2/s
Δt	Simulation time step	s
Δt_c	Stability time step	s
C	Effective heat capacity	J/kgK
c_l	Liquid PCM heat capacity	J/kgK
c_s	Solid PCM heat capacity	J/kgK
θ	Ratio of solid to liquid PCM	-
Q_{irri}	Heat transfer from irrigation	J
$\dot{m}_{HX}$	Mass flow rate of irrigation	m^3/s
$c_{p,w}$	Heat capacity of water	J/kgK
T_{irri}	Irrigation temperature	C
T_{tank}	Tank water temperature	C

CHAPTER 1: Introduction

1.1 Ground Source Heat Pump Performance and Limitations

1.1.1 Geothermal heat pumps

It was estimated that residential and commercial buildings contributed 40% of all United States energy consumption in 2010, 41% of which can be attributed to heating, ventilation, and air conditioning (HVAC) (D&R International 2011). This implies that approximately 17% of the total energy consumption in the United States is a result of residential and commercial HVAC. Furthermore, fossil fuels such as natural gas are often used for space heating. Because of this, HVAC systems contribute to one third of global greenhouse gas emissions (Z. Liu et al. 2017). Energy efficient alternatives to conventional HVAC technology are desired to reduce this energy consumption and reduce greenhouse gas emissions. The geothermal heat pump (GSHP), commonly referred to as ground-source heat pump (GSHP), is the most energy efficient of all HVAC systems. It has a large potential to reduce energy consumption and carbon emissions, on the order of 6 quadrillion Btu per year (Liu et al. 2019). During periods of warm weather, GSHPs operate in cooling mode, pulling heat from the building and rejecting it to the relatively cool ground. Conversely, in cool weather it extracts heat from the relatively warm ground and transfers it to the building. The high efficiency of the GSHP is derived from the working fluid's favorable inlet temperature after circulating through the ground heat exchanger (GHE). This favorable temperature is possible due to the relatively small variation in ground subsurface temperature across seasons (NYSERDA 2017).

1.1.2 Limitations to GSHP implementation

High installation costs are the primary limitation of GSHP implementation. The ground heat exchanger accounts for more than 30% of the installed cost of a ground-source heat pump (GSHP) (NYSERDA 2017). There are generally three categories of ground heat exchangers:

1. Vertical bore ground heat exchangers (VBGHEs)
2. Horizontal ground heat exchangers (HGHEs)
3. Immersed heat exchangers (ponds, lakes, well/groundwater)

Of these three categories, the VBGHE is the most frequently used with 46% of all installations in the United States. HGHEs account for 38%, and the immersed heat exchangers account for the remaining 16% of all installations in the United States (Lund 2001). Conversely, the installation cost of the VBGHE is the highest of the three, while the immersed heat exchangers are the least expensive. This disparity between cost and installation frequency is because the HGHE requires a large amount of land to be installed (NYSERDA 2017). Similarly, using a relatively cheap immersed heat exchanger requires an available pond, lake, river, or ground/well water. These numbers are further skewed by the fact that GSHPs are often chosen by consumers specifically because there is a large area of land or a water source available, which allows for a cheaper immersion HE and reduces the consumer's installation cost. In other words, for the GSHP to reach full market penetration the GHE must be cost-effective, but not require a large amount of land or a water source to operate.

1.2 Reducing the Cost of the VBGHE

Various approaches have been taken to reduce the cost of the GHE. These include improvements to the drilling process, improving the heat exchanger design, and exploring various improvements to the grouting material.

1.2.1 Reducing the drilling cost

The higher cost of the VBGHE is largely due to the high cost of drilling. There are several factors that influence this. One factor is the size of the ground heat exchanger. The GHE must be sized to meet the largest expected peak loads at the minimum expected ground thermal conductivity (GTC). Anything less will result in a failure of the system, which is not acceptable for the consumer. However, this results in a heat exchanger that is oversized, and therefore more expensive, than what is required to meet the heating and cooling requirements for most of the year.

Another factor is the expensive drill that is required to create the deep boreholes for the VBGHE. The equipment used is around 20 years old on average, the cost of such a drill still runs at about $200,0000. A new rotary drill rig can cost as much as $500,000 (Sachs 2002). The cost of drilling per hour is heavily influenced by this cost, as it must be high enough to meet the cost requirements of the equipment price, the associated loan interest, and depreciation value.

Some improvements have been identified as potential areas that can be targeted to shorten the drilling time and reduce the equipment costs. These include an automated drill pipe manipulator, drill rigs that are customized for VBGHE installation, advanced measuring and monitoring systems, and improved power output control for reduced fuel consumption (GEOTeCH 2016).

1.2.2 Improved GHE design

The most commonly used borehole heat exchanger (BHE) is the single U-tube loop, which consists of a single tube that runs down and back up the borehole in a U shape (Liu et. al. 2018). Alternative designs for the BHE exist, including the double U-tube loop, the coaxial loop, and the TWISTER (four U-tube loops twisted together).

Shallow heat exchangers have also been explored, including basket heat exchangers and the GeoColumn. Basket heat exchangers consist of a helical coil wrapped around supports and buried in the soil. These helical coil heat exchangers have the benefit of increased pipe volume per unit depth, which increases the amount of heat that can be transferred for a given depth. This allows for shallow heat exchangers that do not require borehole drill rigs. However, a challenge for this approach is developing drilling methods that can drill moderately deep holes (5-15 meters) at large diameters (greater than 1 ft.). A study by the “Cheap-GSHPs” project developed a technique called “Enlarged Easy Drill” to accomplish this in a cost-effective manner. Results from this study indicate that heating and cooling loads can be handled by basket heat exchangers installed using this technique. The study also found that backfilling with a material with relatively high thermal conductivity can have a significant impact on the temperature response of the heat exchanger (Bertermann et al 2018). This is because the temperature response of the basket heat exchanger is highly sensitive to the ground thermal conductivity. It has a much smaller heat transfer capacity than the VBGHE, so several HEs are required to meet the same loads as a single borehole VBGHE.

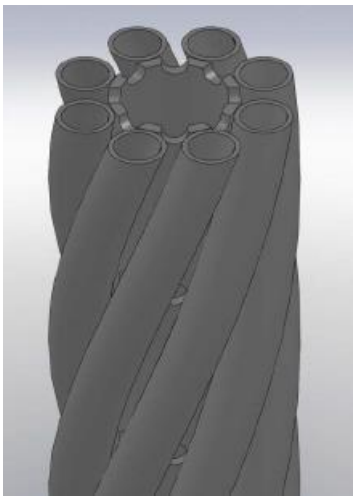

Figure 1. TWISTER heat exchanger design.

The GeoColumn is an innovative approach to the ground heat exchanger that transfers heat to the soil via a shallow tank of water. Figure 2 shows a diagram of the GeoColumn (Cordts 2011). A heat exchanger (HE) consisting of copper coil transfers heat from the working fluid (compressed Freon) to the tank water. Natural convection within the tank generates circulation which improves the convection heat transfer between the water and the HE coils. The most important component of this GHE design is the thermal capacity of the water. This allows for the tank to absorb large amounts of heat energy during periods of peak loads without significantly increasing the tank temperature. This heat is then dissipated to the soil during periods in which the heat pump is not operating, thus returning the tank temperature to thermal equilibrium with the soil. For a conventional GHE, thermal buildup in the soil during peak loads results in a significantly increased HE outlet temperature. In comparison, the large thermal capacity of the tank decreases the HE outlet temperature during periods of peak loads. This results in significantly increased heat pump efficiency compared with a conventional GSHP.

1.2.3 Advanced grouting materials

Backfilling a BHE with thermally enhanced (TE) grout is a well-studied method of achieving increased heat transfer within a borehole heat exchanger. Commercially available bentonite-based grouts are available with thermal conductivities up to 1.6 Btu/hr-ft-°F, a significant improvement over the standard grout (0.38-4.5 Btu/hr-ft-°F) (Tiedje and guo 2013). While it is an effective method of reducing the required BHE size, its effectiveness is highly dependent on the surrounding GTC (Liu et al 2018). This is because a low GTC significantly reduces the impact of the higher conductivity TE grout on the total heat transfer rate. As a result, the cost-effectiveness of the more expensive TE grout is dependent on the GTC of the local soil for a given installation.

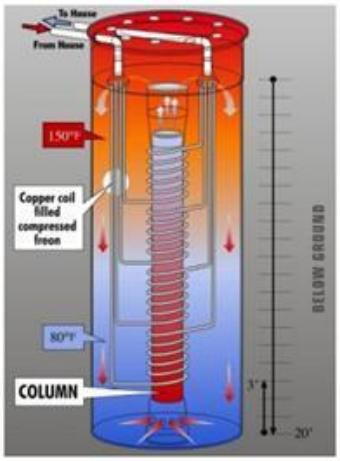

(a) **(b)**

Figure 2. Alternative ground heat exchangers: (a) basket heat exchanger (b) GeoColumn heat exchanger

Another approach which has been investigated is the use of phase-change materials (PCMs) in the BHE grouting material. Studies have shown that the integration of PCMs in backfill material reduces the GHE outlet temperature during peak loads, leading to more energy efficient operation (Bottarelli et al 2015). However, it required that the thermal conductivity of the PCM to be higher than the GTC for benefits to be realized. Also, the cost-benefit may not be sufficient for wide adoption due to the high cost of PCM for relatively small gains in this application.

1.2.4 Evaluation of available improvements

A comprehensive study was conducted to evaluate the impact of available improvements in BHE technology when compared with the conventional approach. This study provided an updated cost model based on national survey data, and utilized the cost model to evaluate the best approaches for decreasing the cost of BHE installation. The study's conclusions were as follows (Liu et al. 2019):

- Implementing thermally-enhanced grout and double U-tube loop in BHE installation were the most cost-effective measures for reducing the borehole length needed to satisfy a given thermal load.
- The effectiveness of BHE improvements is dependent on the ground thermal conductivity. A high GTC allows for a more significant borehole length reduction.
- BHE improvement can result in a reduction of up to 30% in the installed cost of a VBGHE in areas with a high GTC value (> 1.4 Btu/h-ft-°F). However, in areas with a low thermal conductivity value the installed cost may increase.
- Improvements in drilling technology have limited impact (6-16%) on the installed cost and these cost reductions may be eliminated if the drill rig becomes more expensive due to the improvements.

The investigated improvements showed a potential for moderate cost savings potential under certain soil conditions. Most of the previous efforts have focused on improving heat transfer inside the borehole. The small diameter of the borehole limits the potential for increasing the heat transfer, and thereby reducing the cost. It is evident from this study that incremental improvements to GHE technology are unlikely to provide the necessary cost reduction for mass adoption of GSHP technology in the United States. One of the conclusions of this study is that new GHE designs that can provide the same performance while requiring less drilling should be investigated.

1.3 Thermal Energy Storage

1.3.1 Overview

Renewable energy production is a significant and growing resource for reducing carbon emissions. However, sources of renewable energy, such as solar and wind, are often intermittent. This creates a discrepancy between the energy demand and the renewable supply. Figure 3 shows this discrepancy as manifested in California in September 2018. The net demand for energy is the overall demand minus the intermittent renewable output. As is apparent in the figure, the renewable sources do not meet the demand in the early morning and evening as the solar energy is not significant. The energy grid is significantly burdened by this "duck curve" phenomenon, and efforts to reduce this effect can significantly increase overall emissions reductions and cost savings (NREL 2015). Thermal energy storage is one method of addressing this issue. By storing energy during "off-peak" loads in which the electricity demand is small and using that energy during "peak-loads" when the electricity demand is high, the duck curve can be flattened and significant cost and energy savings can be realized. Various thermal energy storage (TES) technologies have been developed for integration with GSHPs, with the primary categories being ice storage, solar collectors, soil, water, and phase change materials.

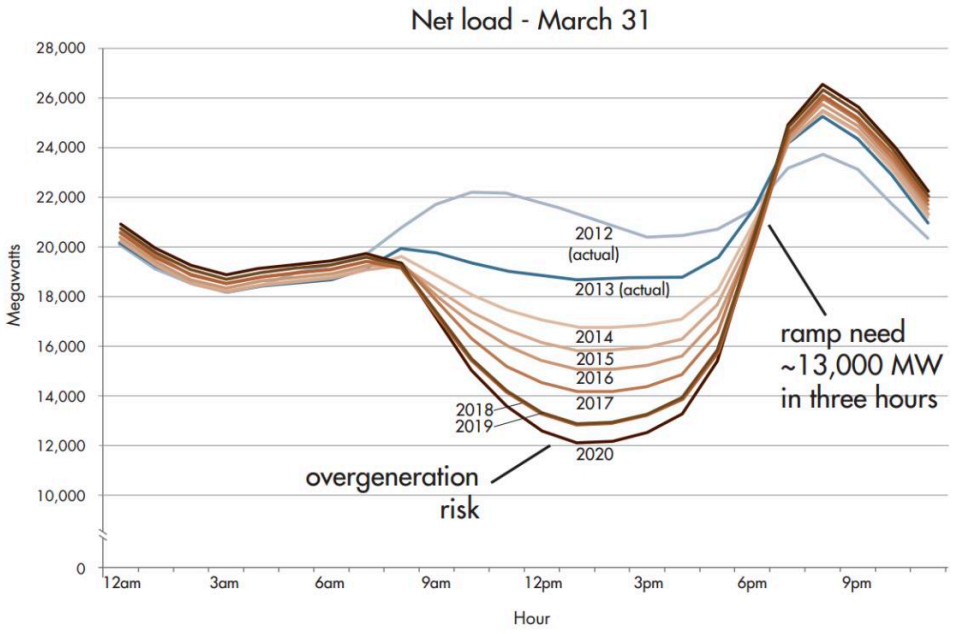

Figure 3. "Duck Curve" of electricity demand due to intermittent renewable power (CAISO 2013).

1.3.2 GSHP integrated with ice storage

For cooling-dominated areas, ice storage can be charged during off-peak hours and then used to provide cooling during peak hours at a much-reduced energy consumption rate. Typically, a chiller is run overnight to freeze water in an insulated tank. This cooling energy is then extracted during peak hours (typically the daytime) to cool the building.

Several studies have investigated the effectiveness of ice storage when integrated with GSHPs. Zhang et al. (2008) studied an integrated GSHP ice storage system for a large commercial building in Beijing, China. After some technical and economical optimizations, they concluded that the installation cost of the system was increased by 107.5% over the traditional system, but the average annual operation cost was decreased by 37.85%. This resulted in a payback period of 4.7 years. Dong et al. (2010) developed a numerical cylindrical heat source model to study the effects of GSHP-ice storage integration on the thermal response of the soil. They found that reducing the number of boreholes and increasing their spacing results in better overall performance. The study also concluded that the operating modes must be well-planned for different conditions to effectively reduce the operational cost.

While the integrated ice storage system is a promising energy-saving technology, the specialized equipment needed to hybridize the GSHP-ice storage system make it expensive and complex. Furthermore, the complex relationship between thermal storage and cooling capacity as they relate to building demands require good design and controls for effective energy-savings.

1.3.3 GSHP integrated with solar energy

In heating dominated areas, solar energy can be stored to assist the GSHP in meeting the heating demands. This is typically done with solar panels and solar collectors. Solar panels store solar radiation in the form of electrical energy which can be used to charge a thermal storage medium. Solar collectors are the most commonly solar energy source that is used in conjunction with GSHP systems. Solar collectors directly solar radiation, which can be used to heat circulating water and charge a thermal storage medium. Typically, the thermal storage medium is the domestic hot water tank. Sometimes, distributed heating in buildings can be controlled to store heat in the building itself. Alternatively, the ground can be used as a thermal storage medium that can be charged with the ground heat exchanger(s).

Many studies have investigated the integration of solar energy and GSHPs. One study found that in heating dominated climates, solar collectors could be used to recharge the ground while still satisfying the cooling demands of the summer. The annual performance was thereby increased by providing a higher temperature to the GSHP system during the winter (Melikyan 1997). An analytical model was developed to predict the performance of a solar assisted GSHP system. The study concluded that solar recharging does not significantly reduce the overall energy consumption due to the energy consumption of auxiliary circulation pumps, etc. However, the installation costs may be reduced as the ability to regenerate the soil temperature allows for shorter boreholes (Eslami-nejad 2011). A hybrid solar assisted GSHP system was studied experimentally in Norway. The study determined that with good control strategy, energy use due to additional circulation pumps could be significantly reduced (Stojanovic 2010).

Wang et al. (2008) studied an experimental solar assisted GSHP with underground thermal storage using a water tank. They found that the size of the water tank and the solar collector size had a large bearing on the

effectiveness of the thermal storage system. In a further study, they concluded that the ratio between tank volume and solar collector area should be in the range of 20-40 $\frac{L}{m^2}$ (Wang 2009). An optimization study was conducted by Kjellson et al. (2010) in which it was posited that the complexity in solar integrated GSHP systems make it difficult to optimize the system design and controls for a given building.

1.3.4 GSHP integrated with water storage

One method of thermal storage that has been investigated is the integration of a thermal storage water tank with a GSHP. The benefit of this type of system is that it can work in mild climates with significant heating and cooling demands. In heating dominated areas, heat can be rejected to the water and stored for use during peak loads. In cooling dominated areas, heat can be extracted from the water and the cooled water can reduce the thermal demands during peak loads. Qi et al. (2010) studied a GSHP system integrated with a water thermal storage system. The system was installed in a commercial building in Beijing, China. The study concluded that the operational costs could be reduced by 13%. The limitation to this approach is that it typically requires a very large water tank to store the thermal energy. Water tank maintenance is also necessary to prevent debris, bacteria, and other unwanted material from reducing the heat transfer performance.

1.3.5 GSHP integrated with PCM storage

Latent heat storage takes advantage of the large amount of energy transfer that is required for a material to change phase from a liquid to a solid, or vice versa. During the phase-change process, the temperature of the material remains relatively constant. This provides a high-energy density at a relatively constant temperature. This minimizes heat loss due to a low temperature gradient while reducing the required storage volume.

Benli and Durmus (2009) and Benli (2011) conducted experimental testing of a GSHP system combined with a PCM thermal storage device for heating a greenhouse and found the system COP to be higher than air-source heat pumps. However, the authors did not isolate the benefit of adding the PCM to the GSHP system. Rabin and Korin (1996) numerically investigated the use of PCM in the form of concentrated annular rings around the ground heat exchanger (GHE). The fluid outlet temperatures were found to be less favorable for GSHP operation compared to the case with no PCM. This is likely due to the low thermal conductivity of the PCM which inhibited heat transfer to the soil. Numerical studies have been performed with PCM used as the grout or backfill material for the ground heat exchanger. These studies showed that PCM can reduce the temperature fluctuation in the ground soil compared to a baseline case. This implies a reduction in the heat transfer rate to the soil on a long-term basis. Also, the spacing of borehole can be reduced, resulting in a reduced land requirement. Bottarelli et al. (2013) investigated the use of a shallow drainage trench for installing a horizontal GHE combined with encapsulated PCMs as a granular filler. The PCMs reduced the seasonal and daily fluctuations in the ground temperature. The PCM also reduced the thermal penetration of the heat into the surrounding soil. Bonamente et al. (2016) compared sensible energy storage using water and latent energy storage using PCMs, coupled with a borehole. Adding the PCMs made the borehole outlet temperature more stable and increased the COP by 2.8%.

1.4 Underground Thermal Battery

The Underground Thermal Battery (UTB) is proposed as a cost-effective alternative to a conventional GHE. The UTB consists of a heat exchanger immersed in a large tank of water buried in the shallow subsurface (< 20 ft. deep) of the soil. Phase-change materials are suspended in the water to increase the heat capacity. The heat exchanger transfers heat from the heat pump loop during cooling loads. This heat warms the tank water, increasing the temperature. The heat input from the HE coils drives natural circulation within the tank, increasing the heat transfer rate between the tank water and the HE coils, PCM, and tank wall while maintaining a relatively uniform tank temperature. The tank has a large heat capacity due to the large sensible heat of water and latent heat of PCMs. This heat capacity reduces the temperature response rate of the tank for a given heat input. Once the tank temperature reaches the phase-change temperature, the PCM begins to melt, absorbing energy and further reducing the temperature response rate. This results in a smaller temperature increase during peak loads than conventional GHEs. This energy can then be diffused to the soil during periods with no cooling loads, effectively distributing the heat transfer of a few hours of cooling loads over a 24-hour period.

The proposed UTB can naturally recharge by transferring heat to the surrounding soil. However, by hybridizing the UTB with other heat sinks or sources the energy-saving capabilities of the UTB may be further increased. Renewable energy sources are one source of thermal energy for hybridization with the UTB. Radiative panels (such as Sky Cool panels) allow for long-wave radiative heat transfer to the atmosphere with no water loss. This could be particularly useful in cooling the UTB during the night in hot climates. Dai et al. (2015) and Girard et al. (2015) conducted experimental analysis of a GSHP coupled with solar collectors. The results indicated that thermal energy from the solar collector could be used to recover the soil temperature, and that the GSHP would operate at a higher overall COP as a result. For this system, the potential for thermal recovery is even greater due to the large heat capacity of the tank.

Another promising avenue of UTB hybridization is the opportunity for active thermal storage. This could be done by connecting a heater and/or chiller to the loop and regenerating the UTB during off-peak demand or when intermittent energy sources, such as solar or wind, are available. The regenerated UTB would then use this favorable temperature to meet future heating or cooling demands with far greater efficiency. By decoupling thermal demands from the electricity grid in this way, the UTB can act as a load-shifting mechanism to reduce peak demands and increase the resiliency of the electric grid.

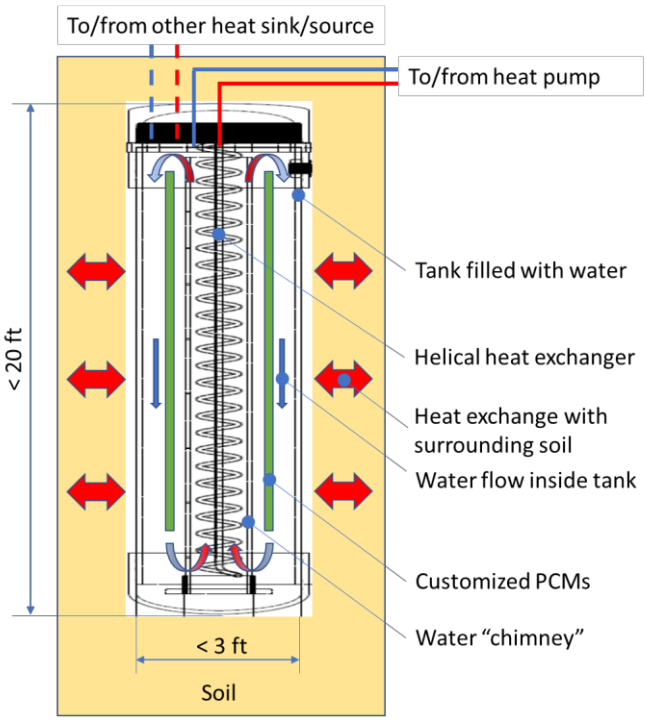

Figure 4. Schematic of UTB prototype concept.

1.5 Objectives and Methodology

The purpose of this study is to evaluate the potential of the UTB as a cost-effective alternative to the convectional VBGHE. This section includes descriptions of the specific objectives and methods for: (1) an experimental study of a UTB prototype, (2) a simplified 1D model of the UTB, and (3) a cost analysis of the UTB installation.

The primary objectives of this study are:

1) to develop a prototype to test the performance of the UTB.
2) to develop a simplified heat transfer model of the UTB to simulate its performance and test various parameters.
3) to develop a cost analysis of an installed UTB and compare it with a VBGHE.

A lab-scale prototype of the UTB is developed along with an apparatus for the simulation of heat pump operation in cooling mode. The experimental apparatus consists of a pump, heater, and instrumentation to measure flow rate and temperature. Temperature measurements are taken throughout the inner tank of the prototype and heat flux measurements at the surface.

A heat transfer model is developed in MATLAB. The model is developed from first principles and is discretized in a one-dimensional cylindrical coordinate system. A phase change algorithm is adapted from the literature to simulate the latent heat transfer of the PCM. An algorithm for the simplified heat balance in the tank is also developed.

A cost analysis is completed using survey data from contractors. Published data is also referenced to support the survey. An itemized cost analysis is proposed as justification for the values presented. The energy cost analysis is compared with the cost premium for various designs to determine the payback period for each. The potential for commercialization is evaluated based on this estimated payback period.

CHAPTER 2: Experimental Study

2.1 Experimental Setup

A lab-scale prototype was developed to test the performance of the UTB. The proposed underground thermal battery is designed for residential applications. In order to evaluate the concept in a laboratory setting, a small-scale prototype was developed. A 1:5 scaling ratio was chosen to scale the device. The dimensions of both the full-scale concept and prototype are presented in Table 1. The mass of the PCM is chosen based on the desired thermal capacity and varies for different testing configurations.

Figure 5 shows a 3-D rendering of the lab-scale UTB prototype. The PCM is suspended in the annulus between the inner and outer tube. An insulative plastic tube is placed around the heat exchanger. This improves the convection heat transfer by introducing a "chimney effect", in which the heat is constrained to a small area, thereby increasing the temperature difference between the top and the bottom of the tank within the tube. This temperature difference creates natural convection that drives the water up the inner tube. Once at the top, the water cools and sinks down the annulus. This circulation significantly improves the heat transfer between the water and the heat exchanger, PCM, and tank wall. The tube also allows thermocouples to be suspended throughout the tank for distributed temperature measurements. In full-scale application, it is planned to use the PCM itself to enclose the coil and produce this chimney effect.

An experimental setup was constructed to test the UTB prototype. Figure 6 shows the schematic of the experimental apparatus for testing of UTB prototype. The experimental apparatus is designed to emulate the operation of a residential GSHP system. The major components include: a circulating pump, heater, rotameter, differential pressure transmitter, and thermocouples. The pump is controlled to circulate water in the helical heat exchanger at a constant flow rate. The heater is insulated to prevent heat loss, and it is controlled by a schedulable power supply that can switch the power on/off in 15 minute intervals. This allows for an approximate emulation of real heat pump operation, which cycles on and off to meet the varying heating or cooling demands of the building. The pressure transmitters measure the pressure difference across the heat exchanger, which effects the power requirement of the pump. The thermocouples measure the temperature difference across the HE, which is used, along with the measured flow rate, to calculate the heat transfer rate of the HE. Figure 7 shows a photo of the actual experimental setup before the prototype UTB is installed in the sand tank. As shown in this figure, four heat flux sensors are installed at the outer surface of the tank. These sensors are evenly distributed along the length of the tank to measure the heat loss through the tank wall.

Table 1. Dimensions of conventional VBGHE and a full-scale UTB.

Dimension	VBGHE borehole	UTB (with 2 tanks)	Ratio (UTB/VBGHE)
Depth (m)	60.96	6.1 X 2	0.2
Diameter (m)	0.15	1.07 X 2	14.3
Volume (m^3)	1.08	2.73 X 2	5.2
Surface Area (m^2)	28.73	10.25 X 2	1.0
Surface area to volume ratio	26.6	3.8	0.2

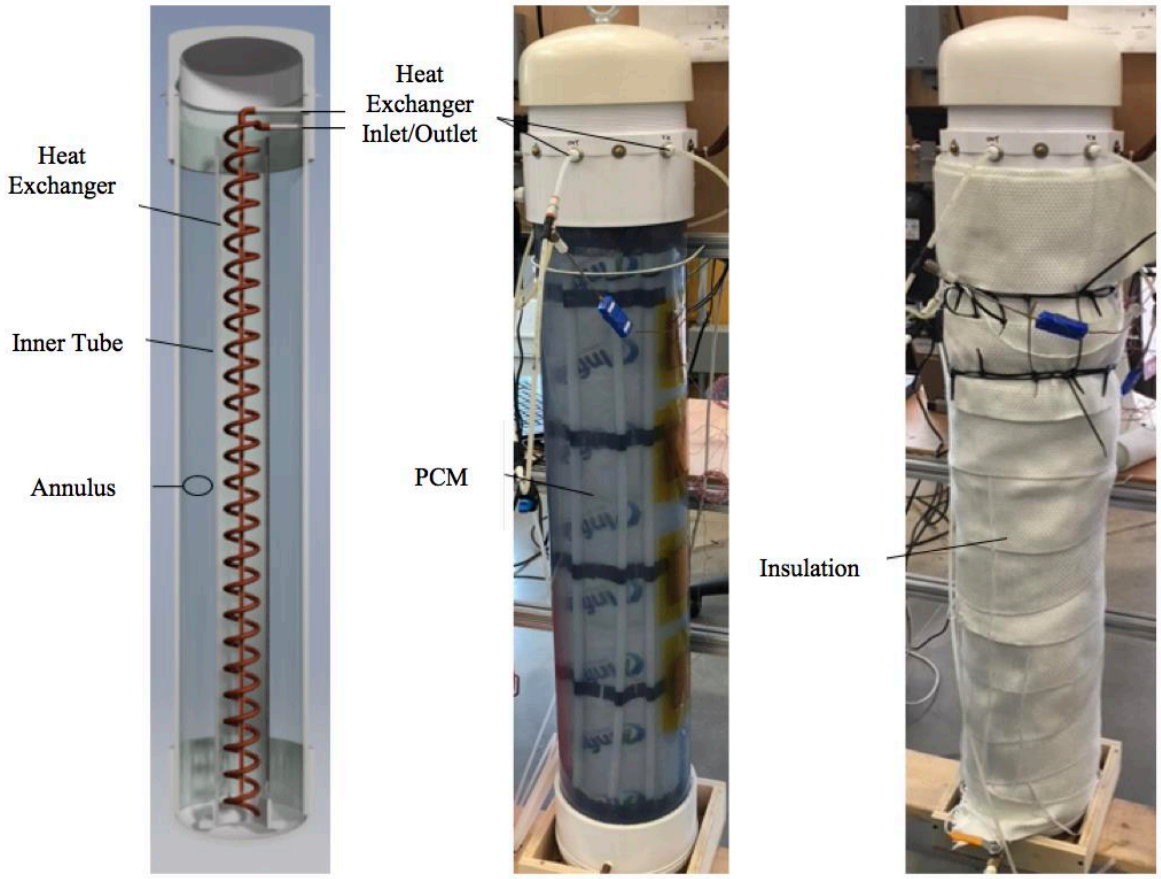

Figure 5. UTB prototype 3-D rendering (left) and actual prototype (center) and insulated prototype (right).

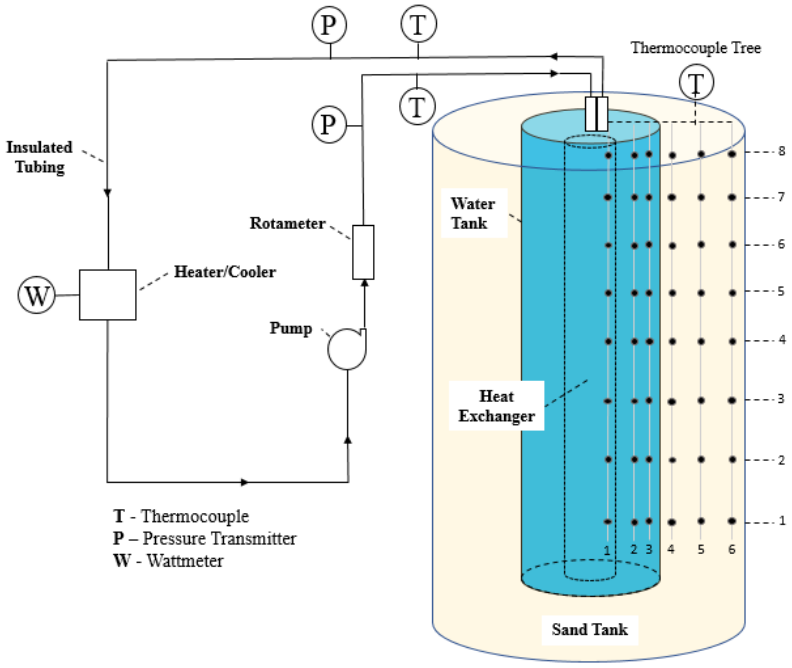

Figure 6. Schematic of the experimental apparatus for testing of UTB prototype.

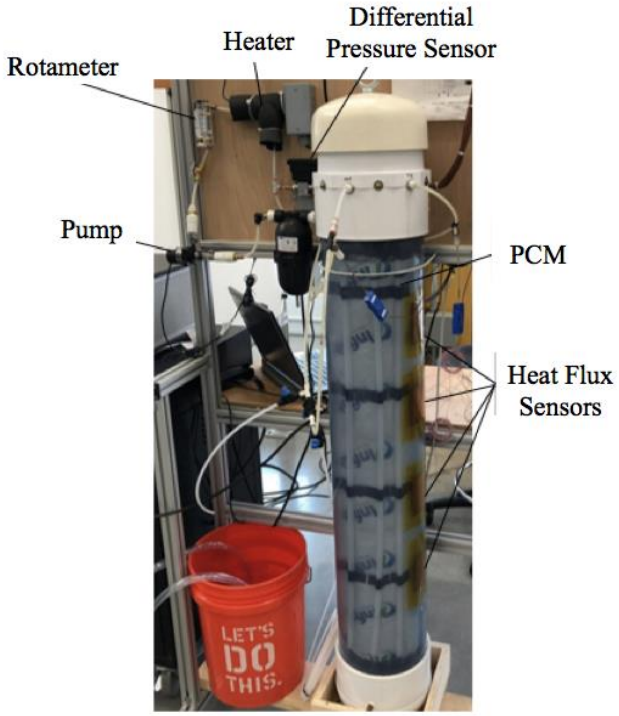

Figure 7. Picture of the actual experimental setup before the prototype UTB is installed in the sand tank

A sand tank (Figure 8) was constructed to emulate the shallow subsurface of the ground. The sand tank is 48" in diameter and 61" tall. Three in-situ tests were performed to measure the thermal conductivity of the sand filled in the tank. The three measured values were 0.501, 0.429, 0.455 W/m-K. This is consistent with published data of dry sand. The outside of the sand tank is insulated to reduce the heat loss during the testing period. A network of 48 temperature sensors is used to measure the temperature profile within the UTB and the sand tank. The temperature sensors are suspended vertically in groups of 8. The first group is suspended inside the inner tube of the UTB, the second in the middle of the UTB annulus, the third on the inside wall of the UTB. The fourth is on the outside wall of the UTB, the fifth is in the center of the sand tank annulus, and the sixth is suspended on the inside wall of the sand tank. They are numbered in a coordinate system which increases radially from the center of the UTB to the edge of the sand tank, and vertically from the bottom of the tank to the top, as shown in Figure 6.

A helical heat exchanger is placed inside the center of the annulus between the tank wall and the UTB prototype. The heat exchanger is connected to a circulating refrigerated and heated water bath. The cold or hot water supplied from the water bath is circulated through the heat exchanger to initialize the sand temperature at the desired level (to emulate ground temperature at different locations). Once the desired temperature at the middle of the annuals (measured with the 5th group temperature sensors) is reached, the circulation of cold or hot water is stopped and the heat is allowed to diffuse throughout the tank until the temperature of the entire sand tank reaches an equilibrium temperature, which is the initial temperature of the sand. Once the desired initial temperature is reached, the heater loop is turned on and run with a prescribed schedule.

2.2 Results

The experimental setup was constructed primarily to validate the assumptions for the concept design of the UTB. These design assumptions include: (1) fully mixed tank temperature due to natural convection in the tank resulting from temperature gradient imposed by the heat exchanger; (2) increased thermal capacity of the tank resulting from phase change of the integrated PCMs; and (3) tank temperature is recovered through heat transfer with the surrounding soil. The validation of these assumptions are addressed in the following sections.

2.2.1 Thermal stratification in the UTB

In order to effectively utilize the heat capacity of the entire prototype UTB, it is important that the water remains well-mixed so that the heat is evenly distributed in the tank. The UTB is designed to facilitate natural convection, which circulates the water and prevents significant thermal stratification. Figure 9 (a) shows the average of the three measured temperatures at each vertical location in the tank, over a testing period. T_mean_1 represents the average of the three thermocouples at the bottom of the tank, and the numbers increase with vertical height (according to Figure 6) until at location 8, which is at the top of the tank (T_mean_8). During the test, the temperature difference between the top and the bottom of the tank remains within 1 ℃, while the average measured tank water temperature increased by 5.5 ℃. The radial temperature distribution in the tank water is shown in Figure 9 (b). MeanTemp_1 represents the average of all the eight measured temperatures at the radial location close to the helical heat exchanger (in the inner tube). MeanTemp_2 and MeanTemp_3 are the vertical average at the middle of the annulus and near the

(a)

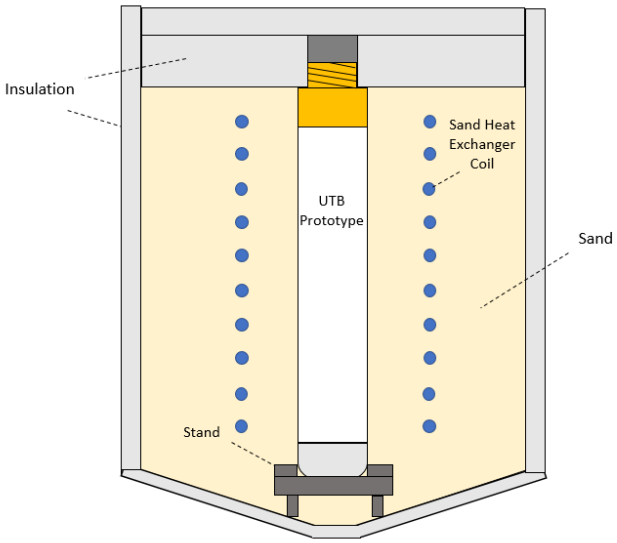

(b) (c)

Figure 8. The sand tank apparatus: (a) prior to being filled with sand; (b) installed with UTB prototype in it (b); and (c) a cross-sectional schematic (c).

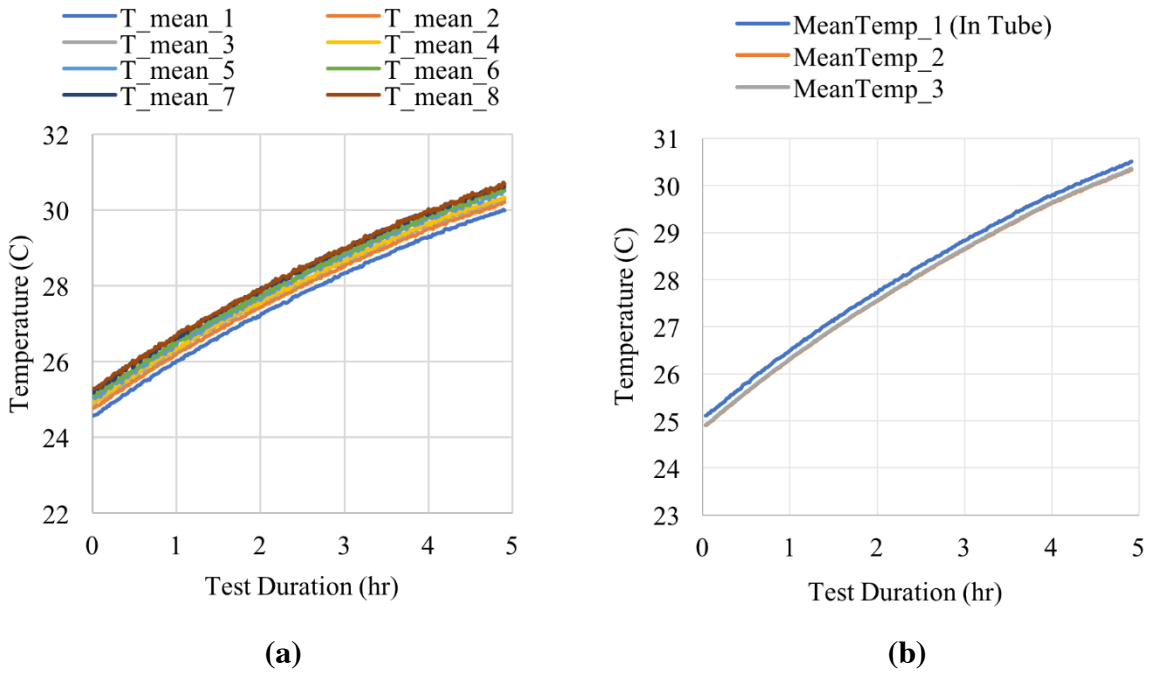

Figure 9. Plot of temperature profile in the UTB prototype: (a) eight temperature measurements evenly distributed in a vertical line in the middle of the annulus between the inner tube and the tank wall; and (b) average temperature along the three vertically placed thermocouple trees.

tank wall, respectively. The temperature difference between the water inside the inner tube and at the tank wall remained within 0.25 ℃ throughout the test, while the overall tank water temperature increased by over 5.5 ℃. This is further evidence of good circulation within the tank, as the heat is effectively transferred from the heat exchanger to the wall of the tank. These results indicate that the tank water is well-mixed in both the vertical and radial direction, which is due to the natural convection introduced by the temperature gradient along the helical heat exchanger.

2.2.2 Evaluation of the Impact of Phase Change Materials on Performance

Three Infinite-R™ PCM blankets with a melting temperature of 23 ℃ were inserted into the prototype UTB in the annulus between the inner tube and the tank wall. As shown in Figure 10, these PCM blankets were separated by spacers, and suspended in the annulus of the prototype UTB, allowing the tank water to circulate between the PCM blankets to facilitate heat transfer. The prototype UTB was wrapped with insulating material to reduce the influence of temperature fluctuations of the ambient air (in the lab) on the temperature of the UTB. Figure 11 shows the average tank water temperature in response to a constant heat input between the UTB with the PCM blankets in it and the same UTB but without any PCM (baseline). For each test, the heater loop ran continuously for 8 hours to provide constant heat input (75 Watts) to the UTBs. For the baseline test, the tank water temperature change was solely determined by the sensible heat of the water. For the comparison case, the tank water temperature was also affected by the latent heat of the PCM when it was melting. The PCM were solid at the beginning of the test when the tank water temperature was below its melting point. As shown in Figure 11, the mean tank water temperature of the UTB with PCMs initially rose slightly above that of the baseline. This is because the sensible heat capacity of the tank

(a) (b)

Figure 10. Pictures of the PCM blankets inserted in the UTB: (a) inside view; and (b) outside view

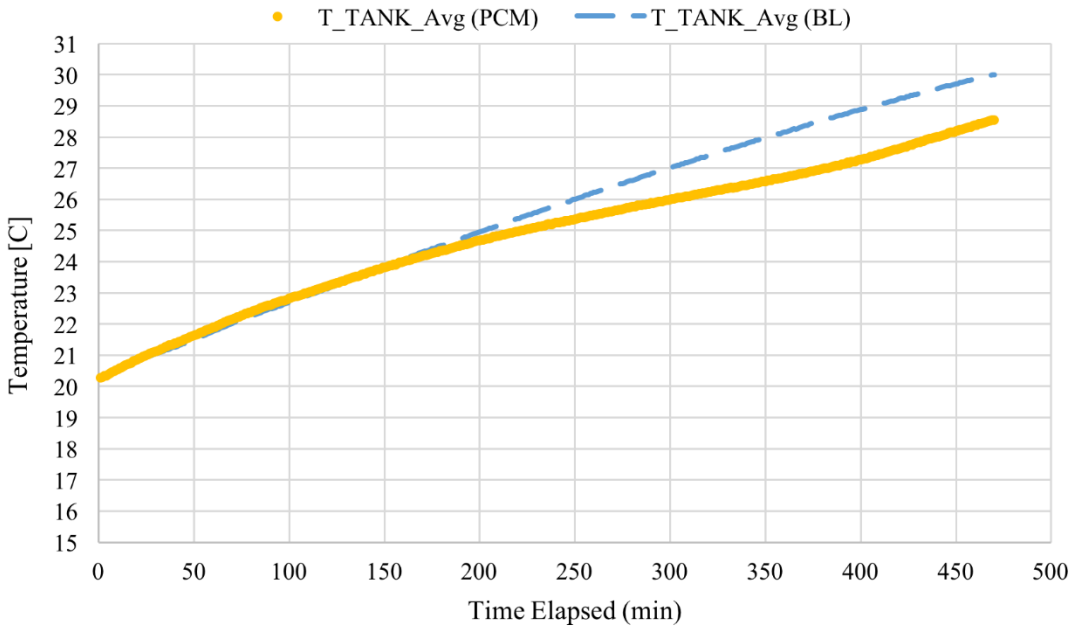

Figure 11. Comparison of the mean tank water temperatures between the baseline and the PCM case.

is slightly decreased because of the PCM blankets and the spacers, which have a lower specific heat than water, replaced some water in the tank. When the tank water temperature rose to approximately 24 ºC, the PCM began to melt. As a result, some of the heat rejected from the heat exchanger was absorbed by the PCM and the slope of the temperature change decreased (since a smaller amount of heat was rejected to the water). This trend continues until all of the PCM was melted, at which point the slope of the temperature change began to match the baseline case. The difference of the mean tank water temperatures between the baseline and PCM case remained at about 1.5 ºC for the remainder of the test.

A heat balance analysis was performed to determine the breakdown of heat transfer in the UTB during this test. As shown in Figure 12, 23% of the heat input was dissipated to the ambient through the tank wall and the insulating material, 45 % of the heat input was absorbed by the water in the tank, and 26% was absorbed by the PCM during the melting process. The total increase of the thermal capacity is calculated based on the total latent and sensible heat of the PCM (L_{PCM} and $Q_{sens,PCM}$) and the heat capacity of the same UTB but with only water in it, for the same temperature change of the tank water:

$$\Delta Q_{cap}\% = \frac{\left(L_{PCM} + Q_{sens,PCM}\right) + Q_{sens,water}}{(Q_{sens})_{Baseline\ case}} - 1$$

The PCM used in this test had a total mass of 4.75 kg and took up about 9% of the total volume of the tank. This amounts to a total latent capacity of 758 kJ, based on the latent heat of the PCM. The total increase in thermal capacity is compared during the period in which phase change occurs, in which the average tank temperature increases from 23 ℃ to 27 ℃ ($\Delta T = 4$ ℃) for the PCM case, and from 23 ℃ to 29 ℃ ($\Delta T = 6$ ℃) for the baseline case. The water was drained and weighed after each test to determine the mass. The specific heat capacity of the water and PCM was taken to be 4.184 $\frac{kJ}{kg℃}$ and 3.53 $\frac{kJ}{kg℃}$, respectively. The addition of PCMs (9% of the total volume of the tank) resulted in a 56% increase in the total thermal capacity of the tank during the period in which phase change occurred.

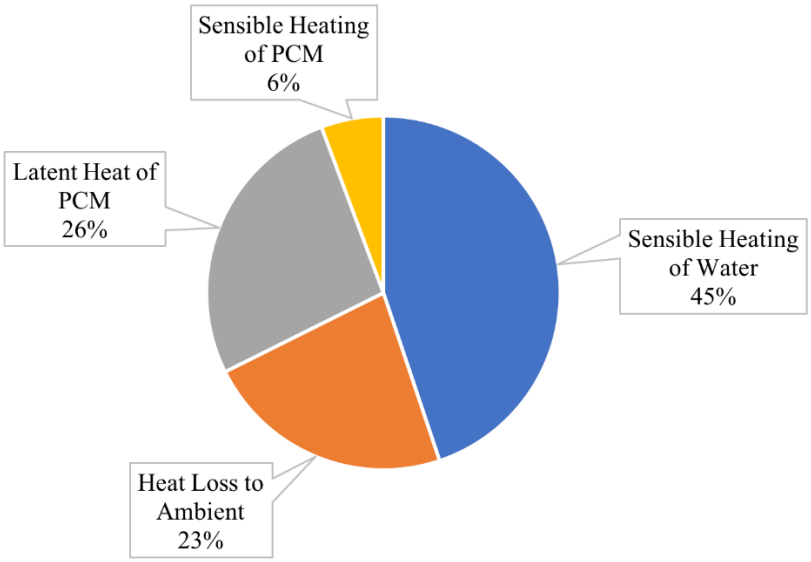

Figure 12. Heat Transfer Distribution by Component of the prototype UTB.

2.2.3 Comparison with a conventional shallow ground heat exchanger

In order to emulate the conventional shallow helical coil ground heat exchanger (a.k.a., the basket heat exchanger), the third test was performed with an identical prototype UTB but filled with sand. The same amount of heat was rejected to the UTB filled with sand. The outlet fluid temperatures of all the three tests (baseline, UTB with PCM, basket heat exchanger) are shown in Figure 13. It is clear from this figure that the outlet fluid temperature of the basket heat exchanger rose much faster than the UTB cases. This is because the basket heat exchanger transfers heat solely through conduction, which resulted in a large temperature gradient between the fluid in the heat exchanger and the surrounding soil. The compact design of the helical heat exchanger results in a relatively large heat flux within a small volume of soil. This quickly warms up the surrounding soil, and in turn the outlet fluid temperature. In contrast, although the water has a low thermal conductivity (similar to the sand), the natural convection of water inside the UTB ensures that the heat capacity of the entire tank water is utilized. It thus slows down the change of tank water temperature for a given heat input. The large heat capacity of UTB allows it to absorb heat during periods with high cooling demands without significant rise of the outlet fluid temperature, and then release the absorbed heat to the ambient (soil) during periods in which there are less demand for cooling. Therefore, it allows for significantly improved heat pump efficiency due to the lower heat pump entering fluid temperature during cooling operation.

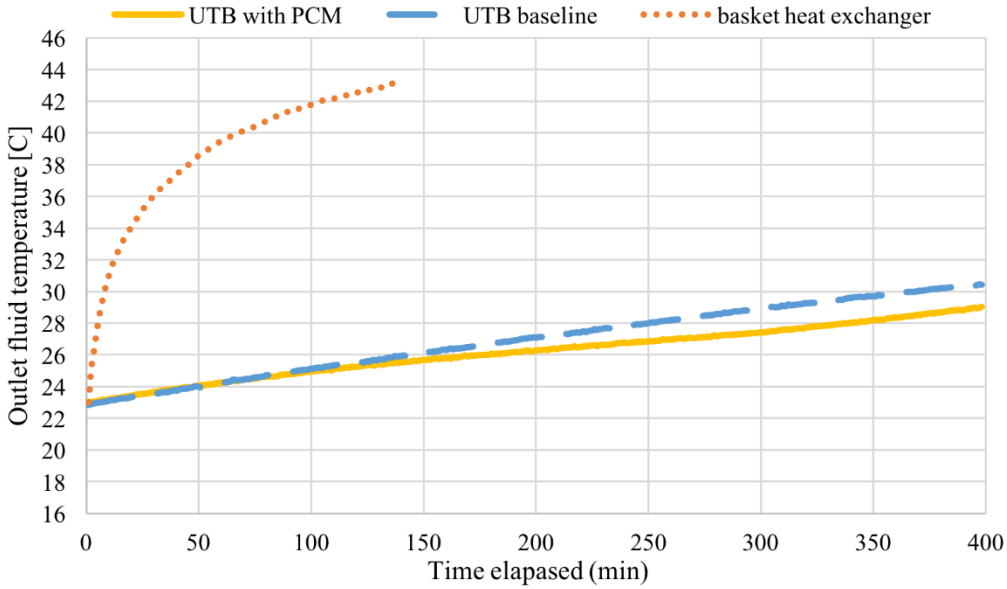

Figure 13. Outlet temperature response of prototype UTB compared with HE in sand.

2.2.4 Evaluation of UTB prototype performance in sand tank

The prototype UTB was immersed in a large sand tank so that it could be evaluated in real soil conditions. The sand tank was initially allowed to remain at the ambient temperature (about 22 ºC). This kept the temperature of the UTB above the melting temperature of the PCM throughout the test, so that no phase change occurred. Once the sand tank reached thermal equilibrium, the heater loop supplied a constant 75 Watts of heat to the heat exchanger in the UTB for 8-hour intervals, and then was turned off for the remaining 16 hours of the day so that the thermal recovery of the UTB could be evaluated.

Figure 14 shows the measurements from this test, including the inlet/outlet fluid temperature of the UTB, average tank temperature, and the average of the eight soil temperature measurements at the UTB surface (#4), middle of the sand tank (#5), and at the wall of the sand tank (#6). As shown in Figure 14, for each of the four days, the heat input was fully rejected to the soil over the 16-hour recovery period and the tank water temperature was recovered after each daily cycle (i.e., returning to its starting point). This demonstrates that the UTB were fully recharged and thus has a repeatable performance in each day.

To enable the melting and freezing cycle of PCMs, the initial sand temperature needs to be reduced and the heat transfer from the ambient should be eliminated. It is planned to add another helical heat exchanger at the outer surface of the sand tank to maintain the temperature at the wall of the sand tank at the desired soil temperature, which emulates the constant undisturbed soil temperature in the shallow subsurface of the ground.

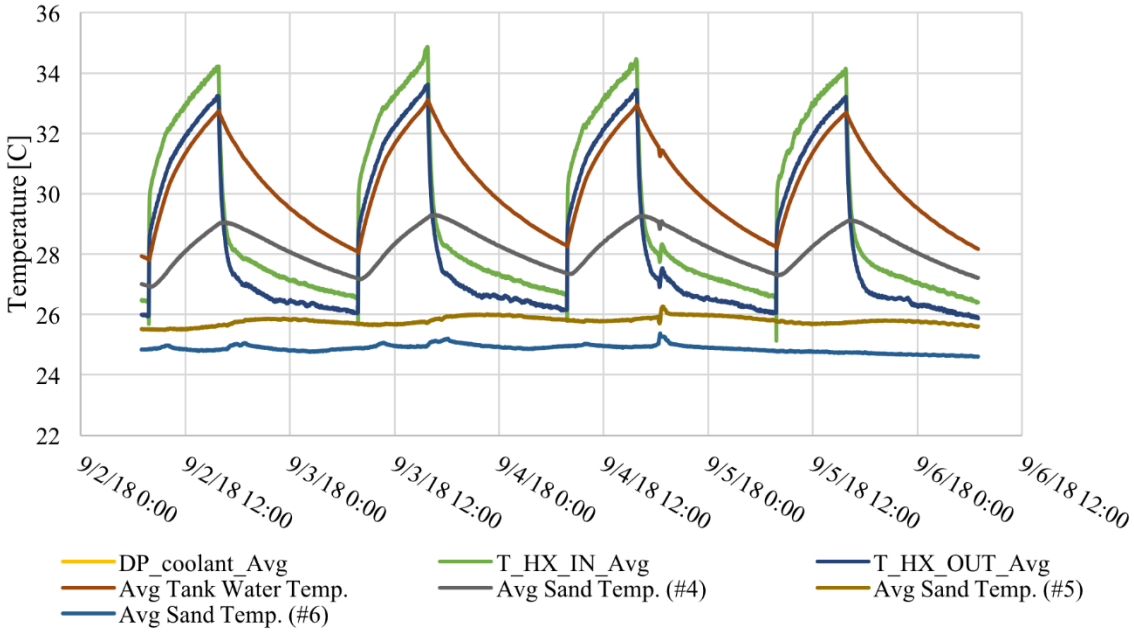

Figure 14. UTB prototype temperature response during Sand Tank test at ambient temp.

2.2.5 Heat exchanger flow rate sensitivity analysis

The internal flow rate of the helical heat exchanger inside the UTB can affect the heat transfer between the heat exchanger and the tank water. It is important to quantify this effect and to determine the optimal design flow rate for the UTB. For this reason, a series of tests were performed in which the flow rate was stepped down from 0.15 GPM to 0.033 GPM. This gave the trend as the flow rate approached the scaled-down design flow rate of 0.024 GPM (1:125 ratio of 3 GPM).

The outlet fluid temperature is an important parameter for the ground heat exchanger design because it will affect the operating efficiency of a ground source heat pump system. As such, an outlet fluid temperature that is closer to the tank water temperature results in better energy efficiency. The optimal outlet temperature is equal to the tank water temperature, as defined in the relationship for the heat exchanger effectiveness:

$$\epsilon_{HXer} = \frac{T_{in} - T_{out}}{T_{in} - T_{tank}}$$

where T_{in} is the inlet fluid temperature, T_{out} is the outlet fluid temperature, and T_{tank} is the temperature of the UTB tank water.

Figure 15 shows the average effectiveness over a 15-minute period of operation at each tested flow rate. The heat exchanger effectiveness decreases with each increase in flow rate. This suggests that a lower flow rate will provide a better performance for this GSHP system. Near the design flow rate, the effectiveness is 0.8. This can be used to guide design considerations for the outlet fluid temperature of the full-scale UTB.

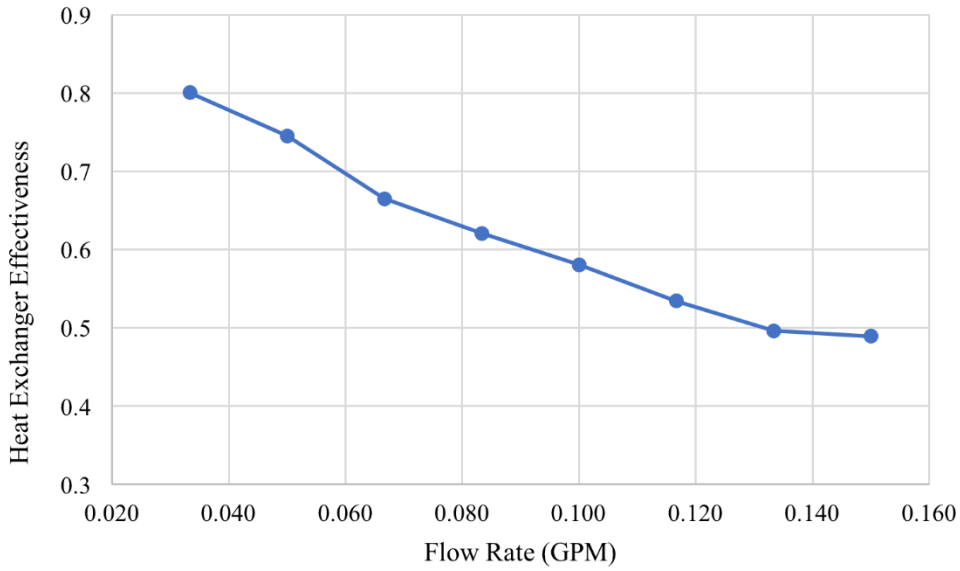

Figure 15. Heat exchanger effectiveness vs. flow rate

2.3 Full-Scale UTB Design

Based on the validations of the UTB prototype, a full-scale prototype has been proposed for in-situ testing. The proposed UTB will consist of a tank, a helical heat exchanger, and a few PCM blankets. The dimensions for the components are listed in Table 2. Figure 16 shows the schematic of the design of a full-scale UTB. Multiple concentric panels constructed from Infinite-R^{TM} PCM blankets are suspended in the UTB. The number of panels is a design parameter that will be varied in the full-scale tests. No inner tube is required, as the PCM panels are used in place of the inner tube to increase the natural convection in the tank. Due to the natural circulation in the tank, no auxiliary pump is required. The design parameters of a UTB for a given application should be optimized to maximize the cost effectiveness of the UTB.

Table 2. Full-scale dimensions for UTB prototype.

Design Parameter	Value
UTB Diameter (ft.)	3.5
UTB Length (ft.)	20
PCM Panel length (ft.)	15
HE diameter (ft.)	1.5
HE length (ft.)	15
# of HE coils	50

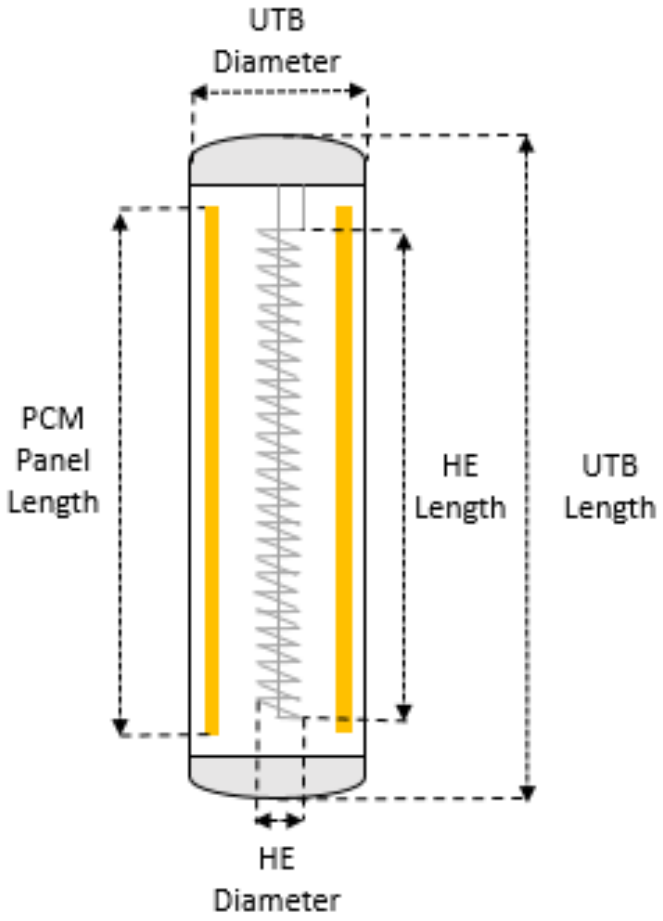

Figure 16. Schematic of the design of a full-scale UTB

CHAPTER 3: Numerical Model

3.1 Model Description

A three-dimensional (3-D) transient heat transfer and fluid dynamic model of the UTB has been developed and validated by Zhang et al. (2019). However, because of the large size of the simulation domain and the detailed numerical calculations of the 3-D model, it is too time consuming to perform long-term (e.g., annual) simulations of the UTB. A simplified version of this model is thus needed to predict long-term performance of the UTB in response to seasonal thermal loads of a GSHP system. A simplified one-dimensional (1-D) transient heat transfer model was developed and validated against the 3-D model. The 1-D model can be used to evaluate the performance of the UTB, and size its components based on the thermal loads and the thermophysical properties of the ground formation.

3.1.1 Assumptions and simplifications

The 1-D model was developed based on following assumptions, which are commonly used for modeling ground heat exchangers:

1. Homogenous and constant thermal properties of the soil, water, and PCM
2. Perfect contact between the UTB wall and the surrounding soil (i.e., no contact resistance)

The model simplified the water tank as a cylinder with uniform temperature. This simplification is consistent with the measured temperature profile inside a small-scale UTB, which was built with a 1: 5 ratio to the dimensions of a full-scale UTB. Figure 17 shows the temperature profile of the UTB during a test when 75 W heat was continuously rejected to the tank for five hours. Figure 17-(a) shows the average of the three temperatures measured in the radial direction—at the center of the tank, in the mid of the annulus between the helical heat exchanger and the tank wall, and adjacent to the tank wall—at various vertical locations in the tank during the test. T_mean_1 represents the average of the three temperature measurements at the bottom of the tank, and the numbers increase with vertical height until at location 8, which is at the top of the tank (T_mean_8). During the test, the temperature difference between the top and the bottom of the tank remains within 1 ℃, while all the measured tank water temperature increased by 5.5 ℃. The radial temperature distribution in the tank is shown in Figure 17 (b). MeanTemp_1 represents the average of all the eight measured temperatures at the radial location at the center of the UTB. MeanTemp_2 and MeanTemp_3 are the vertical average at the middle of the annulus and near the tank wall, respectively. The temperature differences among these vertical averages are within 0.25 ℃ throughout the test, while the overall tank water temperature increased by over 5.5 ℃. These results indicate that the tank water is well-mixed in both the vertical and radial directions because of the natural convection introduced by the temperature gradient along the helical heat exchanger. Therefore, tank was lumped in the vertical and radial coordinates, and was modeled as one single node.

The heat fluxes on the ground surface and the variation of soil temperature along the depth of the UTB were neglected and the annual mean soil temperature (T_m) was taken as an approximation of the initial condition of the simulated soil domain. The heat transfer in the soil is thus lumped in the vertical coordinate and modeled as a 1-D conduction problem. This simplification is based on the fact that the annual variation of the soil temperature decreases drastically with the depth of the soil, as shown in Figure 18. A sensitivity study is presented later in Section 3.3.2 to evaluate the impact of this simplification and its implication on the results of the study.

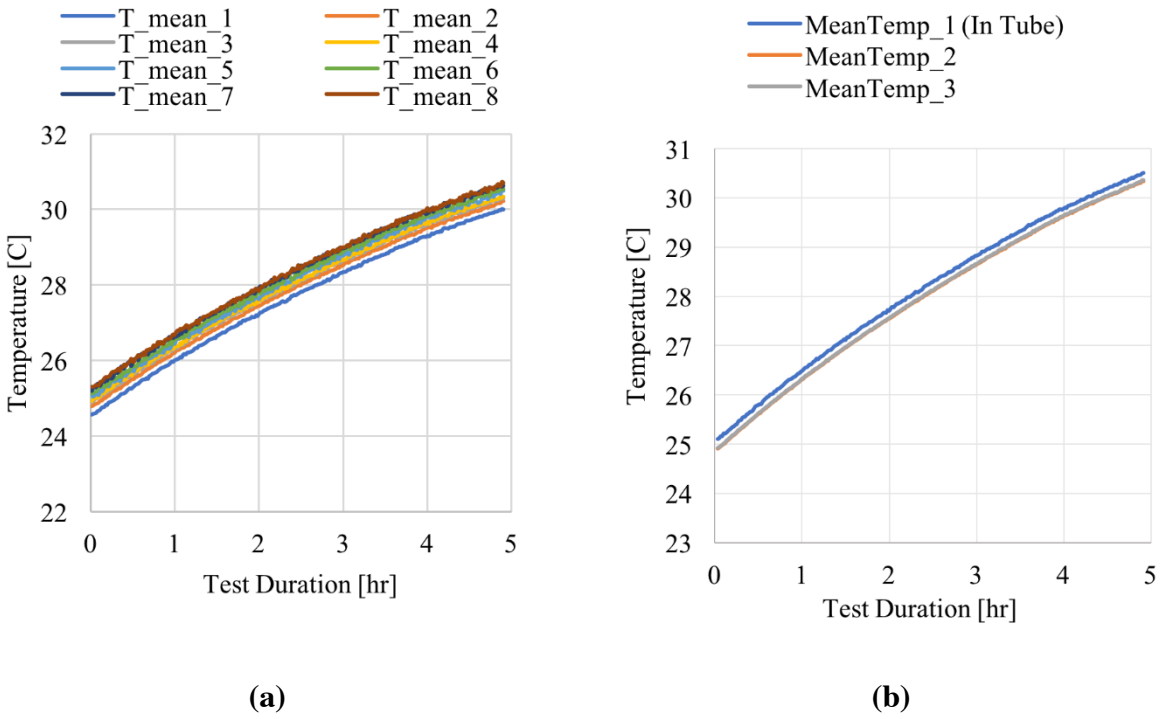

Figure 17. Plot of temperature profile in a small-scale UTB prototype: (a) average temperature measured with three radially placed thermocouples at eight evenly distributed locations from the bottom to the top of the UTB; and (b) average temperatures measured with eight vertically located thermocouples at three radial locations.

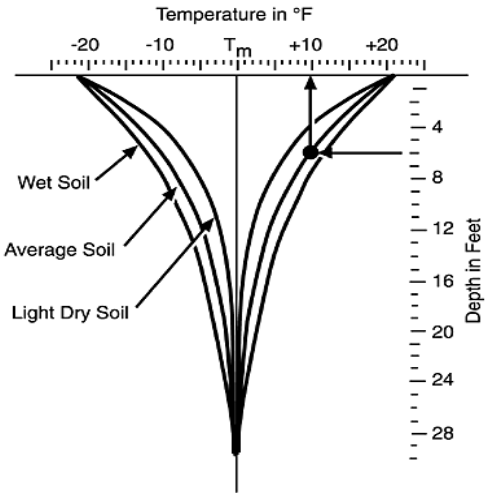

Figure 18. Temperature distribution in subsurface of soil (Cordts 2011).

The heat transfer at the top and bottom of the UTB is simplified by lumping the surface area of the top and bottom of the UTB into the side-wall of the UTB so that the entire surface area of the UTB is modeled at the same temperature gradient between the tank wall and the surrounding soil. This simplification may result in some error in the heat transfer rate to the soil, and consequently the tank water temperature. However, as discussed later in Section 3.3.2, the error resulting from this simplification is not significant. A two-dimensional model that accounts for the vertical temperature profile of the surrounding soil would be needed to more accurately model the heat transfer over the entire surface area of the UTB.

3.1.2 Model structure

The 1-D model consists of two modules—one for the PCM domain and the other is for the soil domain. For both the soil and PCM module, a finite volume method (FVM) is used to calculate the temperature change of each control volume (i.e., a hollow cylinder) at each time step. These modules calculate the heat transfer rate between the tank water and the soil (q_{soil}), and the heat transfer rate between the tank water and the PCM (q_{PCM}). While q_{soil} only includes sensible heat of the soil, q_{PCM} includes both the sensible and latent heat of the PCM when the PCM is changing its phase while exchanging heat with the tank water.

Combining the heat input from the heat exchanger (q_{HEX}) with the heat exchanged with the PCM and the soil, the tank water temperature at a given time step T_i can be calculated with following heat balance equations (Equations 1 and 2). After the new tank temperature is calculated, the next iteration of the time loop begins until the simulation time is complete.

$$\Delta Q = q_{HEX} + q_{PCM} + q_{soil} \tag{1}$$

$$T_i = \frac{\Delta Q}{\rho V_{UTB} c_p} + T_{i-1} \tag{2}$$

where ρ and c are the density and specific heat of water; T_{i-1} is the tank water temperature at the last time step; V_{UTB} is the volume of the tank.

The benefit of this modular structure is that each module can be modeled with different meshes and can be separately changed to model different designs of UTB without affecting the other parts of the model. This flexibility improves the computational efficiency and allows for optimizing the UTB design.

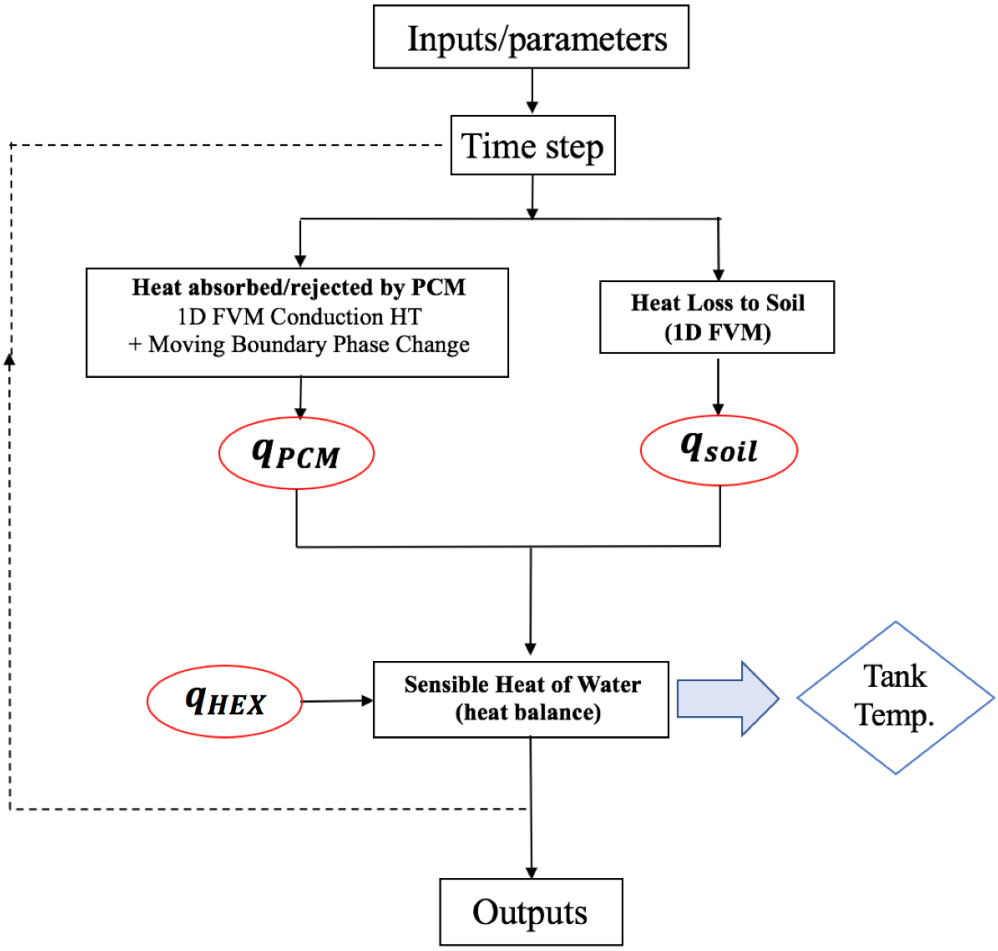

Figure 19. Flow diagram of the UTB model structure.

3.1.3 Simulation domain

The simulation domain of the 1-D model is depicted in Figure 20. The water tank is modelled as a cylinder that has uniform temperature. It connects three subjects, including the helical heat exchanger, the surrounding soil, and the PCM. The heat exchanger provides constant or variable heat input to the tank. The surrounding soil is modelled as a series of hollow cylinders concentric to the UTB. The diameter of the simulated soil domain is 10 times the diameter of the UTB tank so that the heat transfer from the UTB is confined within the simulated soil domain. The boundary conditions for the soil domain consist of a variable temperature boundary at the tank wall, which is equal to the mean tank temperature (T_{tank}); and a constant temperature boundary at the perimeter of the soil domain, which is equal to the mean annual soil temperature ($T_{s,m}$). The soil domain ($\vec{r}_s$) is meshed with a logarithmic node spacing, such that the distance between each node increases as the node position becomes farther from the tank surface (r_1) until it reaches the domain boundary (r_2). This is given by the following expression:

$$\vec{r}_s = \frac{(r_2 - r_1)}{P} * 10^{\vec{u}-1} + r_1 \tag{3}$$

where P is the exponential power of the logarithmic spacing, $\vec{u}$ is a base vector consisting of n_s number of points linearly spaced between the bounds, as given by the MATLAB expression:

$$\vec{u} = linspace(0, log_{10}(P + 1, n_s)) \tag{4}$$

Since the heat transfer rate and the resulting soil temperature change diminishes along the radial direction of the soil domain, this expanding mesh of the soil domain allows for a reduction in the number of nodes without a loss of accuracy, thus reducing computation time. Figure 6 shows a diagram of the simulation domain of the UTB model. The nodes represent temperatures in the domain. The boundary condition of both the PCM and soil domains is a conduction boundary condition with the tank water.

The PCM domain is also modeled as a series of hollow cylinders concentric to the UTB. The mesh of the PCM domain has a linear node spacing given the small thickness of the PCM. The structure of the PCM model will be discussed further in the following sections.

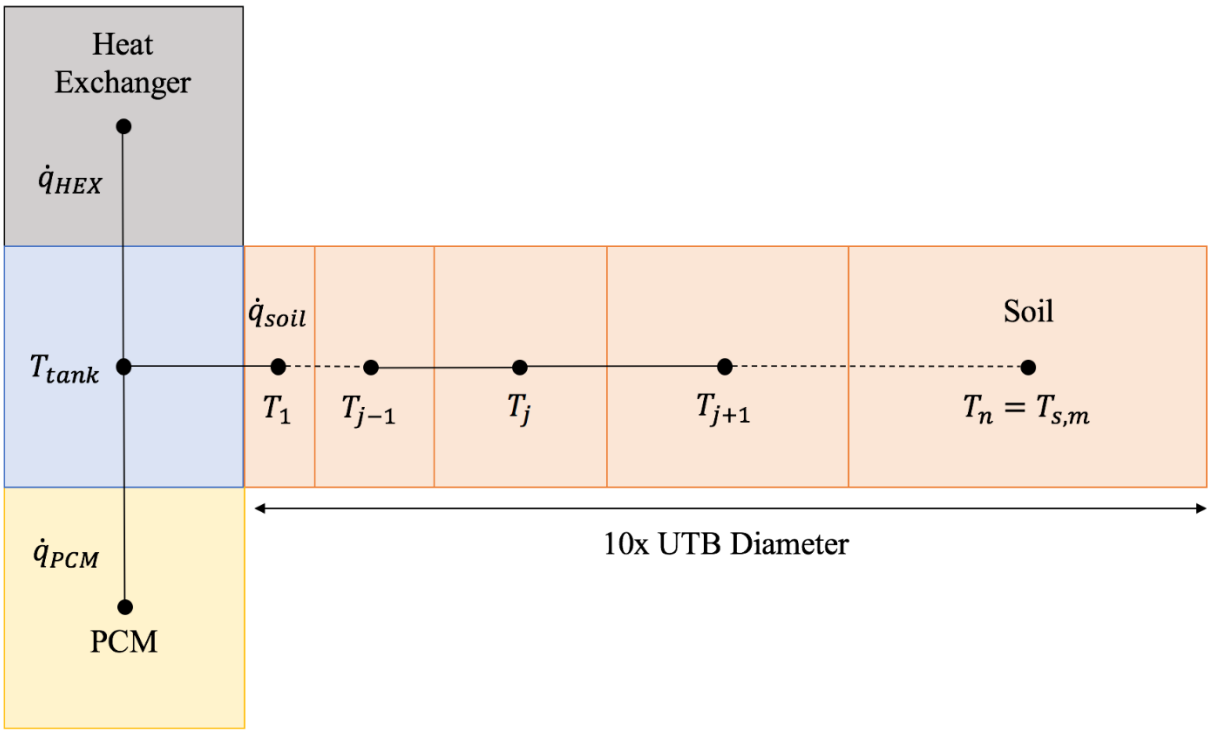

Figure 20. Simulation domain of a one-dimensional model of the underground thermal battery, where j is the spatial index of a soil node, n is the total number of soil nodes.

3.1.4 Governing equations

The governing equations for the conduction heat transfer in the soil and the PCM, as well as the algorithm for modeling the phase change process of the PCM are presented in the following section.

The heat transfer in the soil and PCM is simplified as one dimensional conduction heat transfer along the radial direction, which is expressed below in cylindrical coordinates (Equation 3):

$$\frac{\partial^2 T}{\partial r^2} + \frac{1}{r}\frac{\partial T}{\partial r} = \frac{1}{\alpha}\frac{\partial T}{\partial t} \tag{5}$$

where, T is the temperature of a material (soil or PCM), t is the time, r is the radius from the center of the UTB, and α is the thermal diffusivity of the medium. Discretizing the above equation for explicit numerical calculation gives the following formula:

$$T_j^{i+1} = \alpha \Delta t \left[\frac{T_{j+1}^i - 2T_j^i + T_{j-1}^i}{\Delta r^2} + \frac{1}{r_j}\frac{T_{j+1}^i - T_{j-1}^i}{2\Delta r}\right] + T_j^i \tag{6}$$

where for a cell *j* and time step *i*: Δt is the temporal discretization, Δr is the spatial discretization, and r_j is the radius of the centerline of the cell.

Applying this formula to each finite control volume of the simulated material results in a set of equations. The solution of these equations is the temperature profile of the simulated material at any time step. These equations are solved explicitly based on the calculated temperature profile in the previous time step and the heat fluxes at the current tine step. The size of time step (Δt) is limited by the Cauchy stability criterion as expressed below:

$$\Delta t < \Delta t_c = \frac{1}{2}\frac{\Delta r_{min}{}^2}{\alpha} \tag{7}$$

where Δt_c is the critical time increment, and r_{min} is the minimum spatial increment. As it is desired to calculate the temperatures over a long simulation time, the maximum time step is chosen such that Δt is equal to $0.99\Delta t_c$.

The latent heat accumulation method proposed by Muhieddine et al. (2009) is adapted in this model to account for the latent heat which is released/absorbed during the phase change process. For simplicity, this model assumes that the melting temperature and the solidifying temperature of the simulated PCM are equal, neglecting the sub-cooling effect of some PCMs.

Because the PCM is suspended in the tank water, i.e., exchanging heat with the tank water at both sides of the PCM, two moving phase change interfaces develop within the PCM domain as the PCM temperature reaches its phase changing point and phase change occurs. Each interface is model with a control volume, within which phase change is undergoing at a constant temperature (the phase changing point). The PCM in this control volume is considered to be "mushy", i.e., mixture of solid and liquid PCM. For each time step during the phase change process, the energy transferred into this "mushy" volume is calculated based on a fictitious sensible heat, as expressed with Equation (6):

$$\Delta Q_j = \rho C\left(T_j^i - T_{pc}\right) \tag{8}$$

where, T_j^i is a fictitious temperature of the "mushy" volume; T_{pc} is the phase change point; and C is the effective specific heat of the mixture of solid and liquid PCM, as expressed with Equation (7):

$$C = (1-\theta)c_l + \theta c_s \tag{9}$$

where, θ is the fraction of solid material in the volume. c_l and c_s are the specific heat of the liquid and solid PCM, respectively.

The fictitious sensible heat of this time step is then summed with each subsequent time step until the accumulated heat equals the total latent heat of the PCM in the volume. During this phase change process, the nodal temperature is reset to the phase change temperature after each time step before the temperature of the next control volume (T_{j+1}) is calculated. Once the accumulated heat equals the total latent heat of the PCM in the "mushy" volume, this volume is no longer considered to be changing phase and the standard conduction equation is used to calculate the volume temperature during future time steps. Figure 21 shows a diagram of the PCM domain. In the melting case, the water is warmer than the melting temperature of the PCM. The cells adjacent to the water melt and become liquid. Two "mushy cells" form in which the phase

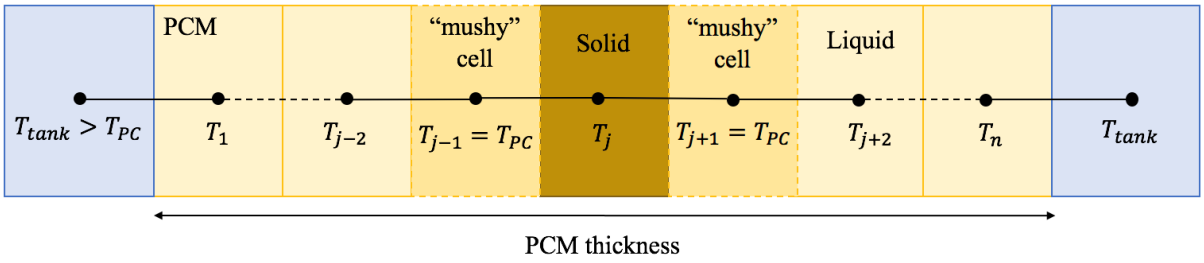

Figure 21. Diagram of PCM domain during phase change process.

change occurs. In between the mushy cells is the solid region which contains the remaining cells. This process is transient and can occur in reverse if the tank temperature drops below the phase change temperature of the PCM.

3.1 Model Validation

3.2.1 Validation against a detailed 3-D model

A 3-D and transient numerical model of the UTB was developed with a commercial software, ANSYS/FLUENT (version 17.2) by Zhang et al. (2019). The simulation domain of this 3-D model is shown in Figure 22. It includes a cylindrical water tank buried in the ground, a helical coil heat exchanger, and a PCM sheet. The helical heat exchanger is located in the center of the tank from the top to the bottom. A PCM sheet is immersed in the annulus between the tank wall and the heat exchanger. The PCM sheet is shorter than the tank so that there is enough space at both the top and bottom of the tank to allow water circulation driven by the natural convection in the tank. The diameter of the simulated soil domain is 10 times the diameter of the UTB and adiabatic conditions are applied to the perimeter of the soil domain. Same as the 1-D model, it is assumed that the thermal properties of the soil, water, and PCM are homogenous and constant, and there is not any contact resistance between the UTB wall and the surrounding soil. The ground-surface heat flux and the soil temperature gradient along the UTB depth are also not modeled with the 3-D model for the reason explained before.

The 3-D model accounts for both the heat transfer and the fluid dynamics within the UTB, as well as the conduction heat transfer in the surrounding soil. It can predict detailed temperature profile in each component of the UTB at any given time. The results of the 3-D model has been validated with experimental data of the small-scale UTB prototype. However, because of the complexity of the numerical calculations and the large size of the simulation domain, the 3-D model is very time consuming and it was only used to predict the short-term (a few days) performance of the UTB (Zhang et al. 2019).

The simulation results of the 3-D model are used to validate the 1-D numerical model. The dimensions and material thermophysical properties of the simulated UTB are presented in Tables 3 and 4, respectively. The initial tank temperature is 295.9 K, just below the 296 K melting temperature of the PCM. The initial soil temperature is 290 K. The heat input to the heat exchanger coil is 4,020 W for the first six hours and there is not any heat input in the following 18 hours.

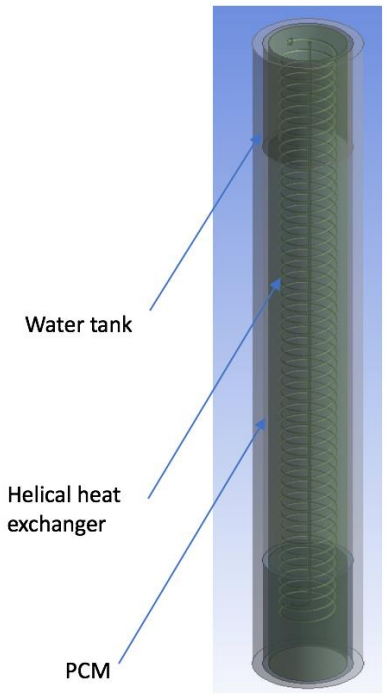

Figure 22. Simulation domain of a three-dimensional detailed numerical model for the UTB.

Table 3. Geometry of the simulated underground thermal battery.

Heat exchanger outer diameter (mm)	Heat exchanger inner diameter (mm)	Helical diameter (mm)	Tank length (m)	Tank diameter (m)	Soil length (m)	Soil diameter (m)	PCM thickness (mm)	PCM length (m)
28.85	22.45	381	6.71	0.76	7.93	7.62	80	4.47

Table 4. Materials thermophysical properties of the simulated underground thermal battery.

	Soil	Water	PCM	Copper
λ (W/(m·K))	1.72	0.6	1.09(solid)/0.54(liquid)	387.6
c_p (J/kg/K)	2121	4182	3140	381
ρ (kg/m^3)	1900	998	831.3	8978
T_{melt} (K)	--	--	296	--
L (kJ/kg)	--	--	200	--

Figure 23 shows that the tank water temperature predicted by the 1-D model matches that predicted by the 3-D model well. The highest tank water temperature predicted by the 1-D model is 297.5 K, which is only 0.1 K higher than that predicted by the 3-D model. The Root Mean Square Error (RMSE) between the tank temperatures predicted by the two models is 0.09 K during the 24-hour time period.

Figure 24 shows the liquid fraction, defined as the ratio of liquid to solid in the simulated PCM domain, predicted by each model through the 24-hour simulation period. The 1-D model under-predicts the melting rate of the PCM relative to the prediction of the 3-D Model. This disparity is consistent with the small difference in tank temperature predicted by the two models—with lower melting rate of PCM, more heat is absorbed by the tank water, which resulted in higher tank water temperature predicted by the 1-D model. The discrepancy in the predicted liquid fraction may be due to the different algorithms for modeling the phase change process employed by the two models. It should be noted that the difference in the predicted tank temperature is very small and therefore the 1-D model is acceptable for predicting the long-term performance of the UTB.

3.1 Annual Simulation Results

3.3.1 UTB vs. conventional VBGHE

Annual simulations of the UTB was conducted to investigate its performance in response to thermal loads of a typical residential GSHP system. Figure 25 shows the leaving fluid temperature of a conventional VBGHE and that of a UTB, which has two parallel connected water tanks. Dimensions of the simulated UTB and the VBGHE are listed in Table 5.

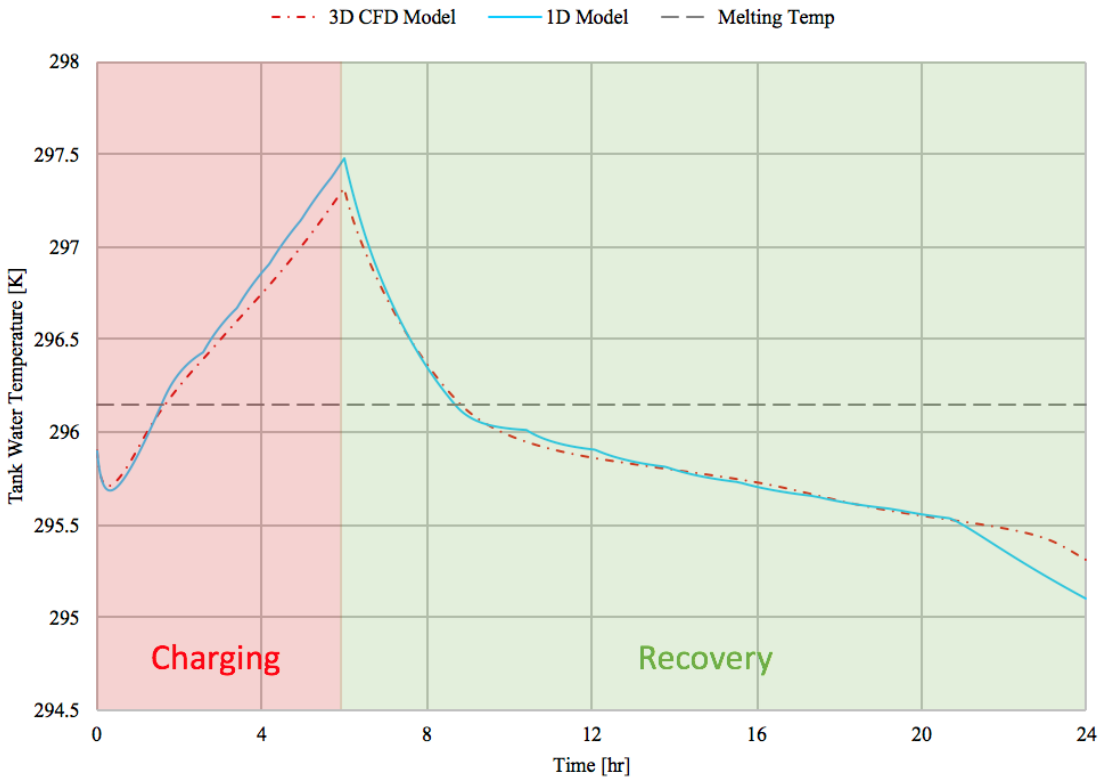

Figure 23. Temperature profiles for phase change simulation with 1D and CFD Model.

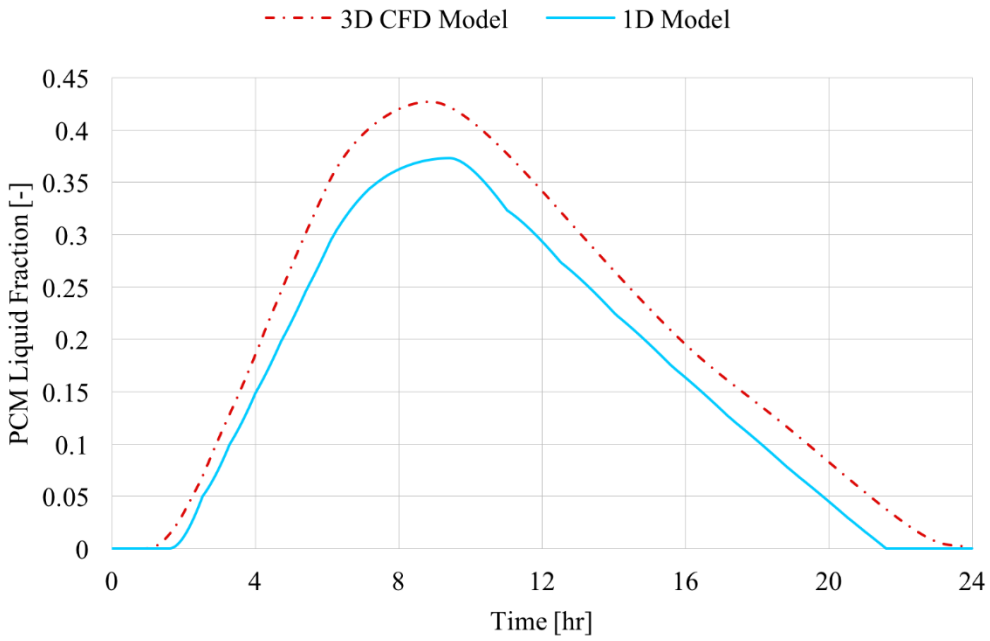

Figure 24. Liquid Fraction for phase change simulation of 1D and CFD UTB models.

Table 5. Dimensions of conventional VBGHE and a full-scale UTB.

Dimension	VBGHE borehole	UTB (with 2 tanks)	Ratio (UTB/VBGHE)
Depth (m)	60.96	6.1 X 2	0.2
Diameter (m)	0.15	0.76 X 2	10.2
Volume (m^3)	1.08	2.77 X 2	5.1
Surface Area (m^2)	28.73	14.56 X 2	1.0
Surface area to volume ratio	26.6	5.26	0.2

The ground thermal conductivity is moderate—2.63 W/m-K. The simulation is conducted using hourly thermal load of a residential GSHP system with 1-ton capacity in Knoxville, TN. The thermal load is predicted using a widely-accepted building energy simulation program, eQUEST version 3.6 (Hirsch and Gates 2017). The leaving fluid temperature of the VBGHE is also predicted with eQUEST. As shown in Figure 25, the leaving fluid temperature of the UTB varies within a small range during daily operation. However, because of the relatively low temperature difference between the tank water and the surrounding soil, UTB exchanges heat with the ground at a lower rate than the conventional VBGHE. As a result, the thermal buildup in the tank causes the leaving fluid temperature of the UTB to increase over time. Despite the thermal buildup, the maximum leaving fluid temperature of the UTB is still comparable with that of the VBGHE in this case. Furthermore, the annual energy consumption of the GSHP system using the UTB is 2-5% less than that using the conventional VBGHE.

It was expected that the PCM would melt and freeze in a daily cycle during the summer as the UTB's temperature fluctuated. However, once the water temperature rose above the melting temperature of the PCM it remained there for several months, as shown in Figure 26, due to continues heat rejection from the GSHP unit. This suggests that the PCM will not naturally cycle on its own, and may therefore only be useful in applications in which there is active regeneration of the UTB tank temperature so that the PCM can be cycled between melting and freezing on daily basis.

For a more detailed look into the behavior of the UTB, the leaving fluid temperatures of the UTB and the VBGHE in one week in each season is presented in Figure 27. In January [Figure 27 (a)], the UTB temperature stays flat with little variation, while the VBGHE fluctuates significantly with the changing thermal loads. In March [Figure 27 (b)], the fluctuations of the two temperature are more similar, but there are occasional jumps in the VBGHE temperature due to switching from heating to cooling mode. The leaving fluid temperature of the UTB is lower than that of the VBGHE in March due to slower heat extraction rate of the UTB. In July [Figure 27 (c)], the leaving fluid temperature of the UTB is lower than that of the VBGHE, which is due to the stored cooling energy in the UTB and the slower increase of the tank temperature. In October [Figure 27 (d)], the leaving fluid temperature of the VBGHE fluctuates much more significantly than the UTB in response to the frequent switching between heating and cooling operation of the GSHP unit. The stable leaving fluid temperature of the UTB results in more energy efficient operation of the GSHP unit.

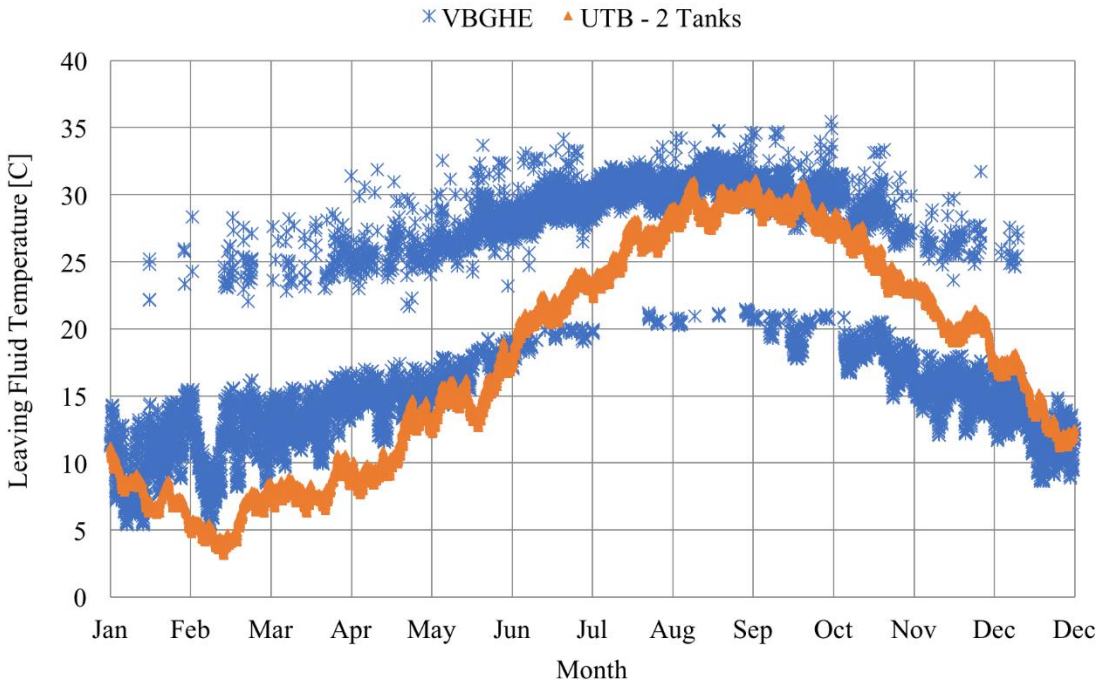

Figure 25. Comparison of simulation-predicted leaving fluid temperature between a UTB (with 2 tank) and a VBGHE during a one-year operation in Knoxville, TN and with moderate ground thermal conductivity.

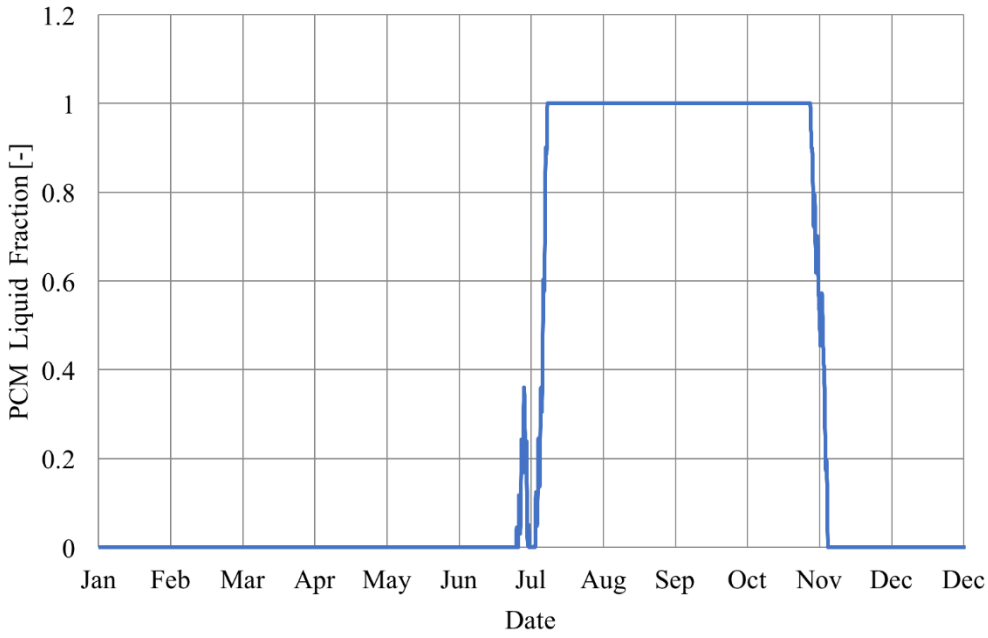

Figure 26. Liquid Fraction of PCM during a one-year operation in Knoxville, TN and with moderate ground thermal conductivity.

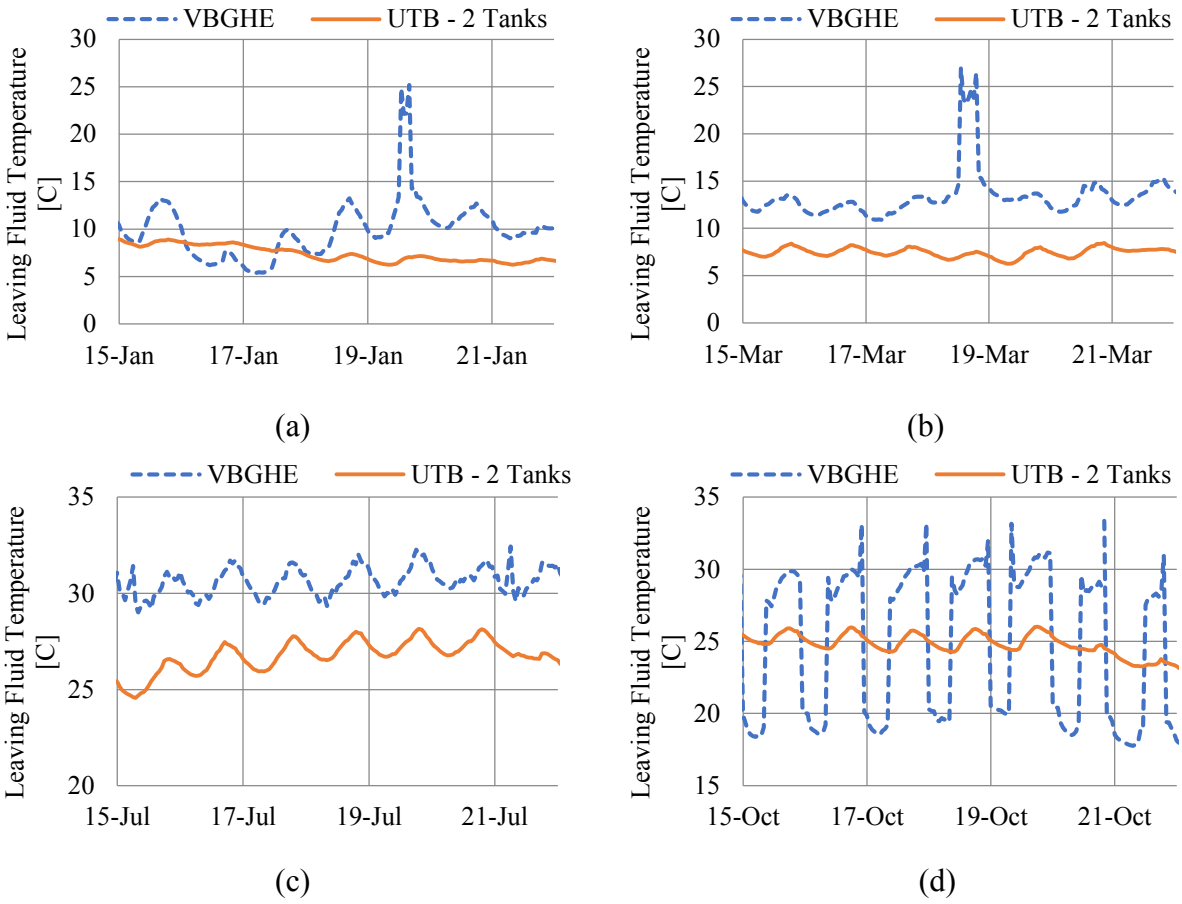

Figure 27. Comparison between the leaving fluid temperature of the UTB and the VBGHE in one week of each season: (a) winter, (b) spring, (c) summer, (d) fall.

3.3.2 Impact of soil temperature

As discussed in Section 3.1, there is some seasonal variations in the soil temperature where the depth is less than 6-7 m. The magnitude of the temperature variation decreases along the depth of the soil. A series of simulations were performed to assess the impact that this temperature variation could have on the UTB performance predicted by the 1-D model. In these simulations, the soil thermal conductivity is 2.63 W/m-K and the simulation-predicted thermal loads of the 1-ton residential GSHP system in Knoxville, TN was used. Figure 28 shows the leaving fluid temperatures of a UTB resulting from three different soil temperatures. The high and low soil temperatures correspond to the reasonable bounds of the average soil temperature along the depth of the UTB during a year. Because of the time lag of the soil temperature change compared with the ambient temperature (Kursuda Equation), the highest soil temperature usually occurs a couple of months later than the peak of the ambient temperature. Therefore, the actual maximum UTB leaving fluid temperature may be lower than that predicted with the high end of the soil temperature, which is 5°C higher than that predicted using the annual mean soil temperature. Considering the maximum leaving fluid temperature of the conventional VBGHE is also 5°C higher than that from UTB, it is likely that the actual maximum leaving fluid temperature of the UTB would be similar to that of the VBGHE when the variation of soil temperature is accounted for. To more accurately predict the leaving fluid temperature of a UTB, a 2-D model of the soil domain is needed to account for the spatial and temporal variations of the soil temperature.

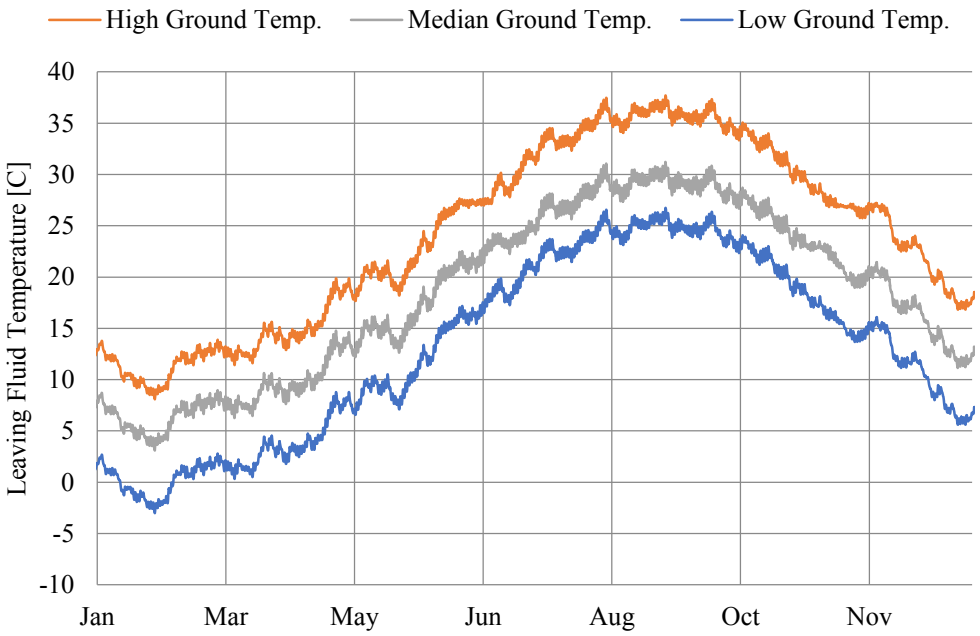

Figure 28. Leaving fluid temperatures of a UTB resulting from low, mean, and high soil temperatures during a one-year operation in Knoxville, TN and with moderate ground thermal conductivity.

3.3.3 Impacts of key design parameters

A parametric study was conducted using the 1-D model to evaluate the performance of the UTB in various operating conditions. The goals of this study include: (1) determine the optimal UTB configuration for meeting the thermal loads under various investigated conditions; and (2) evaluate the effectiveness of the PCM for increasing the thermal capacity of the UTB.

For this study, thermal loads for a residential building in Oklahoma City, OK and Knoxville, TN were used. Oklahoma City has a higher cooling load and a higher annual mean soil temperature (16.7ºC) than Knoxville, TN (15.6ºC). Three soil thermal conductivities (TCs) were investigated for each location. These ranged from low to high values: 1.72, 2.63, and 3.46 W/m-K (other properties are the same as listed in Table 4). Furthermore, a variety of UTB design configurations were simulated: a single large tank with a diameter of 3.5 ft. and a depth of 22 ft., a set of two tanks with a smaller diameter of 2.5 ft. and the same depth of 22 ft., and four small tanks with a diameter of 1.25 ft. and a depth of 22 ft. Another case, a four tank UTB with double PCM, was also investigated. For each case except the last one, the total mass of the PCM in the tanks was kept constant at approximately 850 kg. The PCM was assumed to be in the form of ¾" think panels suspended in the tank water.

There are six base cases corresponding to the two thermal load profiles (KNX and OKC) and the three thermal conductivities. For each case, four different configurations of the UTB, with dimensions listed in Table 6, were simulated and compared with the conventional VBGHE. The heat pump electricity consumption was estimated using a simple heat pump model, which calculates the heat pump power consumption based on performance curves of the heat pump, the hourly thermal loads of the building, and the predicted entering water temperature (i.e., the leaving fluid temperature of the UTB). The results of the parametric study indicate that a UTB with similar borehole surface area to the traditional VBGHE can have similar or even lower maximum leaving fluid temperature than that of the VBGHE, assuming moderate to high ground thermal conductivity. In the case of a two- or four-tank UTB in places with moderate to high ground thermal conductivity, the average annual heat pump energy consumption was reduced by 3% compared with that resulting from using the VBGHE. Figure 29 shows a comparison of the annual heat pump electricity consumption between the various configurations of the UTB for the three ground thermal conductivities in Knoxville, TN. This graph shows that the UTB with a single tank fails to match the performance of the VBGHE, but it may still be a viable option in moderate to mild climates and with favorable ground thermal conductivities. There was not a significant improvement in performance between the four-tank and two-tank UTB configurations (when the total surface areas are the same), which suggests that the surface area is the most significant design factor for the UTB. Also noteworthy is the fact that doubling the PCM does not improve the performance for this design because the PCM does not cycle frequently during the summer.

Table 6. Dimensions of conventional VBGHE and four UTB configurations

Dimension	VBGHE borehole	UTB (with 1 tanks)	UTB (with 2 tanks)	UTB (with 4 tanks)	UTB (with 4 tanks and large PCM)
Depth (m)	60.96	6.1	6.1 X 2	6.1 X 4	6.1 X 4
Diameter (m)	0.15	1.07	0.76 X 2	0.381 X 4	0.381 X 4
Volume (m^3)	1.08	5.49	2.77 X 2	0.696 X 4	0.696 X 4
Surface Area (m^2)	28.73	20.5	14.56 X 2	7.3 X 4	7.3 X 4
Surface area to volume ratio	26.6	3.7	5.3	10.5	10.5
PCM volume (m^3)	-	1.02	0.51 X 2	0.26 X 4	0.26 X 4

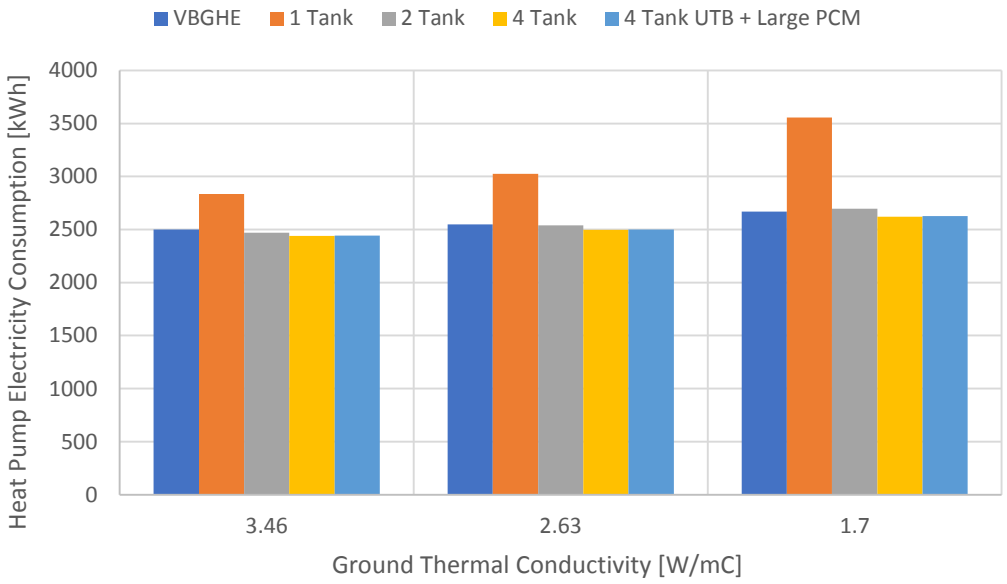

Figure 29. Comparison of annual heat pump electricity consumption between various UTB configurations and a VBGHE under varying thermal ground thermal conductivities in Knoxville, TN.

Figure 30 shows the maximum annual leaving fluid temperature of a UTB with two tanks and a VBGHE in Oklahoma City and Knoxville at the three thermal ground thermal conductivities. In the OKC case, which has a high cooling demand, the VBGHE outperforms the UTB in all but the high ground thermal conductivity. However, in the KNX case, which has a moderate cooling load, the UTB outperforms the VBGHE in all cases, particularly with a moderate or high ground thermal conductivity. This suggests that the UTB is more sensitive to the operating conditions than the VBGHE, and performs significantly better in favorable conditions. Under highly favorable conditions, it is possible that the UTB may have significantly higher performance than the VBGHE.

Figure 31 shows the annual heat pump electricity consumption for a VBGHE and a UTB with two tanks for the three ground thermal conductivities. These results show that in the moderate Knoxville climate the UTB has a similar performance to the VBGHE in all ground thermal conductivities. However, in extreme conditions such as the hot OKC climate with low thermal conductivity, the UTB may have significantly poorer performance than the VBGHE due to thermal buildup in the tank. The variation between annual heat pump electricity consumption in different ground thermal conductivities is not highly significant under moderate thermal loads. For the UTB with two tanks in Knoxville, there is an 8% increase in annual electricity consumption between the low and high ground thermal conductivity. This suggests that with proper sizing the ground thermal conductivity does not significantly affect the performance of the UTB.

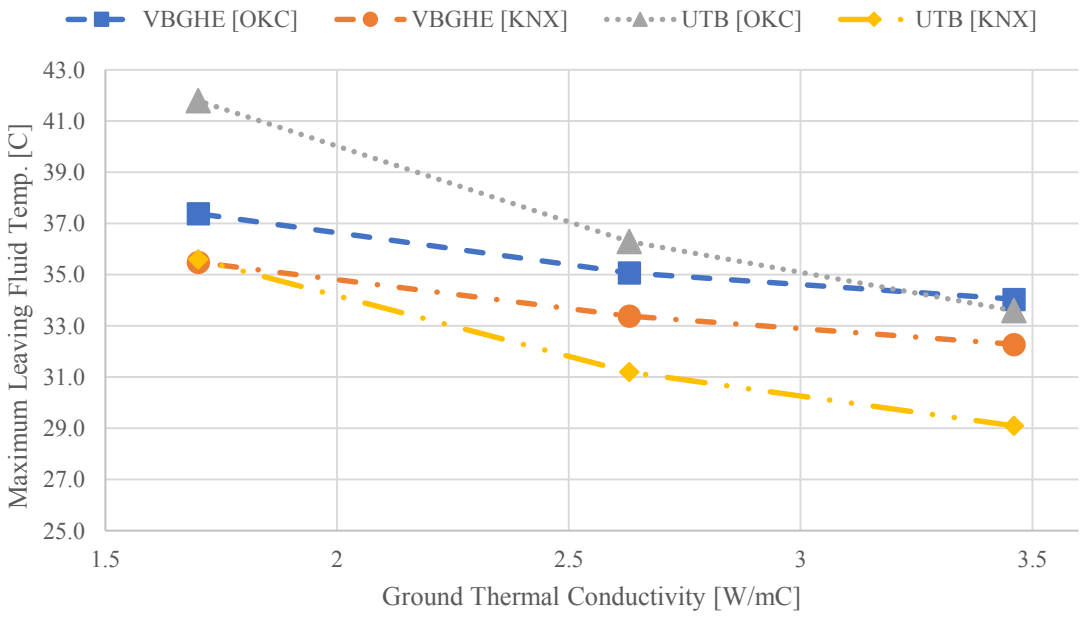

Figure 30. Comparison of the maximum leaving fluid temperature between a VBGHE and a UTB with two tanks under various operating conditions.

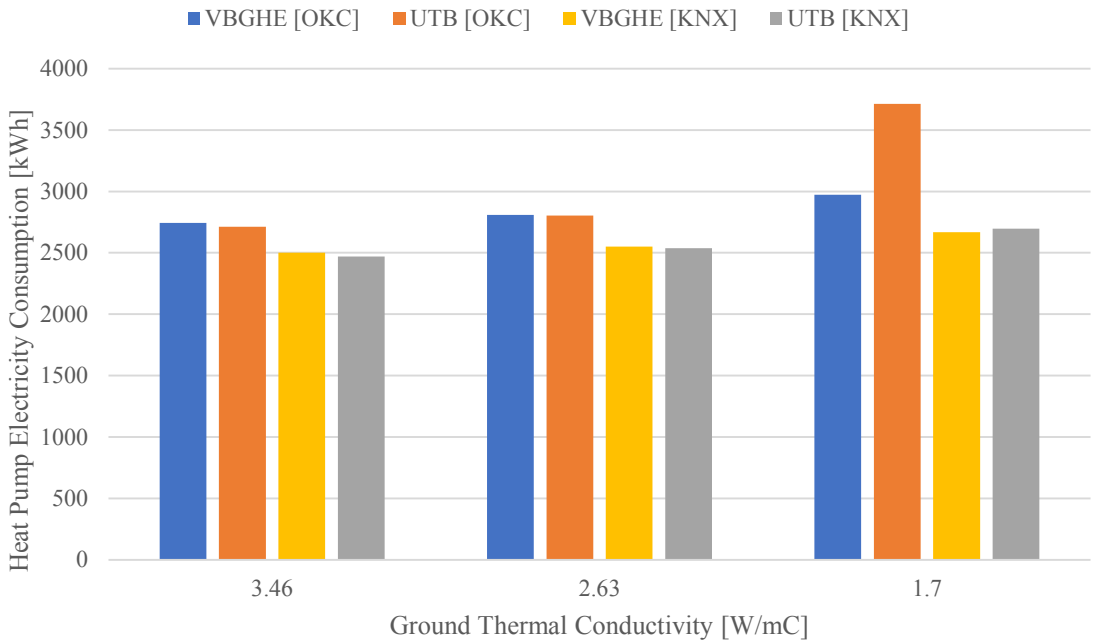

Figure 31. Comparison of the annual heat pump electricity consumption between a VBGHE and a UTB with two tanks under various operating conditions.

3.3.4 UTB Integrated with an irrigation system

One advantage of the UTB over the conventional VBGHE is its larger thermal capacity due to the mass of water and the PCM in the tank. The large thermal capacity can be used to store heating or cooling energy that would normally be wasted. The relatively cool municipal water consumed for lawn irrigation in many residences can be used to replace the warm water the UTB during the hot summer months. This is useful in hotter climates, were the UTB may struggle to meet the cooling demands with excessive thermal buildup in the tank. The integration with the irrigation system is simple—the municipal water goes into the UTB to flush out the warm water in the UTB, which is used for irrigation and the cool municipal water stays in the tank. This is modelled as a simple mixing problem, in which inlet water is mixed with the remaining tank water to reduce the tank water temperature at a given time step.

For this simulation, the thermal loads from Oklahoma City were used to simulate the UTB. The ground thermal conductivity was taken to be a moderate 2.63 W/m-K, and the annual mean soil temperature was 16.7°C. The simulated irrigation system was a single sprinkler head system with a 5/8" hose. The flow rate from the hose under the pressure of the municipal water supply is approximately 16 GPM (Water Resource Foundation 2016). The outlet water from the UTB tank is sent to the sprinkler head. This water flow is in an open loop configuration and it is separated from the helical heat exchanger, which is connected to the GSHP unit in a close-loop configuration. The heat flux from the open loop heat exchanger is calculated as:

$$Q_{irri} = \dot{m}_{HX} c_{p,w} (T_{irri} - T_{tank}) \quad (10)$$

where, $\dot{m}_{HX}$ is the mass flow rate of the irrigation system, $c_{p,w}$ is the specific heat of water, T_{irri} is the city water temperature, and T_{tank} is the tank water temperature at the current time step.

Because the mass of the tank is large relative to the mass flow of inlet water for a given time step, no iteration is required and the outlet temperature which flows out of the tank to the sprinkler head is assumed to be the tank temperature at the current time step. The new tank temperature is calculated from the heat balance between the state of the tank at the current time step and the inlet heat flux from the irrigation:

$$\mathrm{T_{i,new}} = \frac{Q_{irri}}{\rho \mathrm{V_{UTB}} \mathrm{c_p}} + \mathrm{T_{i,old}} \tag{11}$$

where, $\mathrm{T_{i,old}}$ is the tank temperature at the current time step after calculating the heat transfer to the soil and PCM.

The irrigation schedule was based on a set of controls that were designed to approximate real irrigation needs, while optimizing performance. First, the open loop heat exchanger only operated when the temperature of the tank water was higher than the municipal water. The municipal water temperature was approximated as the monthly average of the dry bulb temperature of the ambient air at Oklahoma City. Secondly, the irrigation frequency was varied based on the month of the year as would be expected based on typical lawn operation for the weather. The exact schedule is shown in Table 7 below. The average dry bulb temperature for each month is also shown.

Figure 32 shows the results of this study, with a comparison between the non-irrigation and irrigation cases for a single- and two-tank UTB. A single-tank UTB would normally fail under these conditions due to its small surface area and the thermal buildup in the tank. However, when coupled with an irrigation system the single-tank UTB becomes functional. Due to the influx of cool water to the tank, the PCM can cycle more frequently, which maintains a low temperature in the tank. Although the overall energy consumption is still higher than that resulting from using the VBGHE by approximately 13%, the potential of reduced cost could make the single-tank UTB an attractive alternative to the VBGHE. It should be noted that the performance is sensitive to the PCM phase-change temperature. If the phase-change temperature is too high it will not provide a significant benefit and if it is too low the tank water temperature will not be able to re-freeze the PCM for future use. For a two-tank UTB, integration with a pre-existing irrigation system can further improve the performance. It should be noted that the integration with a pre-existing irrigation system will not increase the water consumption.

Table 7. Irrigation frequency and estimated municipal water temperature by month.

	Jan	Feb	Mar	Apr	May	Jun	Jul	Aug	Sep	Oct	Nov	Dec
Irrigation frequency	Off	Off	Off	Every Three Days	Every Three Days	Every Two Days	Every Two Days	Every Two Days	Every Three Days	Off	Off	Off
Avg. Dry Bulb Temp. [F]	33.6	44.2	50.8	61.2	69.2	77.0	81.9	82.2	73.5	62.6	49.6	38.5

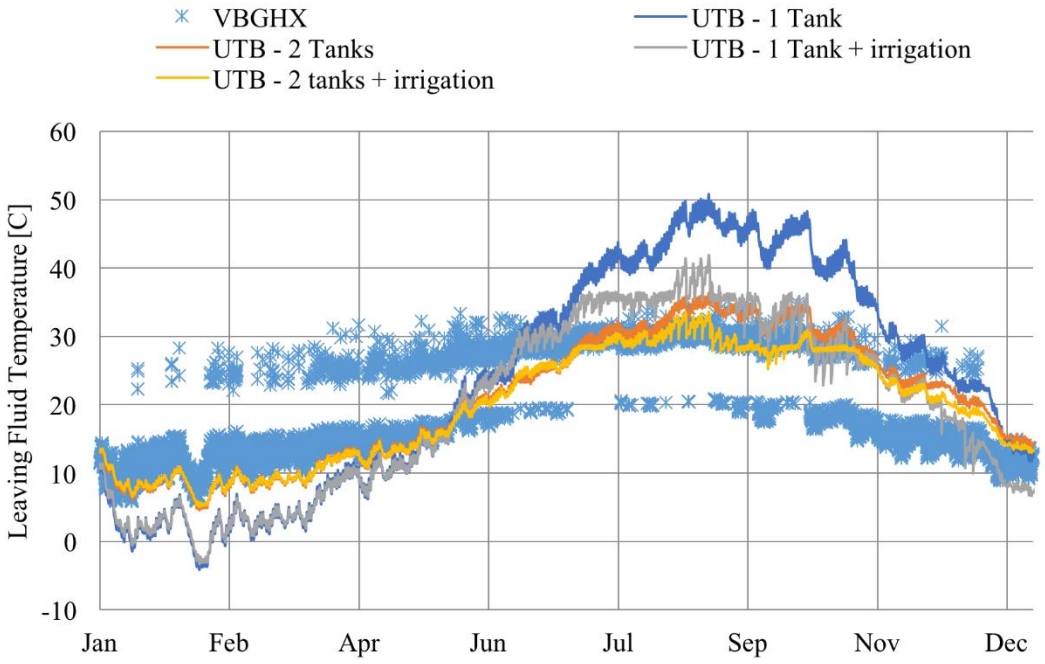

Figure 32. Comparison of leaving fluid temperature of various designs of UTB and that of the VBGHE during a one-year operation in Oklahoma City, OK and with moderate ground thermal conductivity.

CHAPTER 4: Cost Analysis

4.1 Cost Model

In order to determine the cost-saving potential of the UTB, a cost model has been developed. Table 8 gives the base cost data from which the cost model will be constructed. This cost data includes retail prices for components as well as estimates for contractor work including drilling and installation. Corrugated ADS pipe is chosen as the base material for the construction of the UTB tank. The listed pipe diameters are nominal diameters and correspond to slightly larger ODs, with 36" corresponding to a real diameter of 42" and 24" corresponding to a real diameter of 28". Auger drilling is separated into two cases, one which includes a stainless-steel casing for support of the hole and one which does not. The estimated VBGHE installation is based on a somewhat rocky ground formation as would be found in Knoxville, TN.

4.2 UTB Cost Estimate

4.2.1 Auger drilling with casing

When digging a hole with an auger drill, stainless-steel casing can be used to support the hole and prevent collapse. This is especially necessary in cases in which the hole needs to be permanent, such as in the construction of wells. This casing adds significantly to the cost of drilling because of the high cost of the stainless-steel materials. However, it is not always necessary. In this case, the UTB tank supports the hole walls after digging. Because of this, casing would only be needed in situations where the hole would collapse on itself immediately before the UTB could be installed. For this analysis, both casing and no-casing scenarios will be analyzed.

A baseline design of a UTB is needed to quantify the cost of installation. The design must have a capacity that is approximately equivalent to a conventional VBGHE for the same heat pump capacity. Based on the results presented in Chapter 4, we can conclude that the UTB with two tanks can meet this requirement for most thermal load profiles and ground thermal conductivities. This design consists of two UTB tanks with a diameter of 2.5 ft. and a depth of 20 ft. They are buried approximately 2 ft. below the ground surface, for a total hole depth of 44 ft.

Table 8. Cost data for full-scale UTB.

Item	Unit Price	Supplier Type	Source
Corrugated Pipe 36"	$836.99	Retail	(Agrisupply, 2019)
Corrugated Pipe 24"	$454.99	Retail	(Agrisupply, 2019)
Helical Coil (3/4" PVC)	$139 /100 ft.	Retail	(McMaster Carr, 2019)
Auger Drilling (with casing)	$61 /ft.	Contractor	(RSMeans 2010)
Auger Drilling (without casing)	$21 /ft.	Contractor	(RSMeans 2010)
VBGHE installation	$16 /ft.	Contractor	(Liu et al. 2019)

For drilling in which casing is required, the average drilling cost is $61 per foot (RSMeans 2010). This gives a drilling cost of $2684 for the UTB with two tanks. The components of the UTB consist of a corrugated pipe which acts as the tank wall, a PVC helical coil for the heat exchanger, and various components to connect the heat exchanger and seal the tank. The 24" nominal diameter corrugated pipe is priced at $455 /20 ft. (Agrisupply, 2019. This gives a total pipe cost of $908 for the UTB tank. The required heat exchanger tubing is estimated to be 100 ft. per ton of cooling capacity, which gives a heat exchanger cost of $139. Miscellaneous components, such as caps and connectors, are estimated to be 5% of the cost of the tank and heat exchanger. A 20% markup is added to the components for auxiliary components and labor (assembly), at a cost of $109 for the UTB with two tanks. The PCM is neglected from this cost analysis due to its ineffectiveness in this design, as shown in Chapter 4. Summing these costs gives a total estimated cost of $3731 for a UTB with two tanks in the scenario in which the drilling requires casing. This represents a 17% cost increase over the conventional VBGHE.

The original design for the UTB consisted of a single large tank. While this may not be feasible under some operating conditions, there is a potential for a favorable cost-benefit in some situations. This is particularly true in favorable conditions or when there is the ability to refresh the tank using pre-existing sources such as irrigation. The single tank UTB consists of the same components as the two tank UTB, only the tank is larger at 36" in nominal diameter. At a cost of $61 per foot, the total drilling cost is $1118 for a 22 ft. hole. The total cost of the components is $1128. This includes $837 for the 36" corrugated pipe, $139 for the heat exchanger, $49 for auxiliary components, and a 20% markup on the components for assembly. Summing these values gives a total cost of about $2318 for the UTB with a single tank. This is a significant 28% cost reduction over the conventional VBGHE.

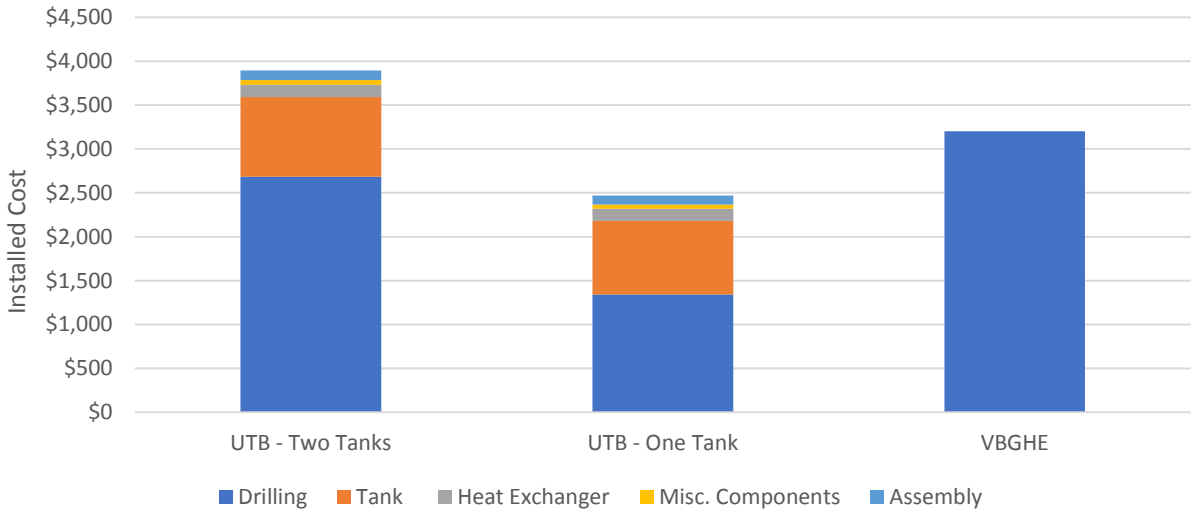

Figure 33. Cost comparison for UTBs installed using auger drilling with casing.

4.2.2 Auger drilling without casing

For drilling in which casing is not required, the average drilling cost is $21 per foot (RSMeans 2010). This gives a drilling cost of $924 for the UTB with two tanks. The total installed cost of the two tank UTB is reduced to $2016 in this scenario, which represents a cost savings of 31% over the VBGHE. For the single tank UTB, the cost is even lower. The drilling for a single 22 ft. deep hole is $462, giving a total cost of $1473. This represents a cost savings of 49% over the VBGHE.

4.3 GHSP System Cost

For a residential HVAC system, the capacity is typically 2-4 tons depending on the size of the residence. For this analysis, a small residential home with a cooling capacity of 2 tons is considered.

To develop a full cost of the GSHP system, the ductwork and heat pump equipment must also be accounted for. The cost of ductwork is estimated as $2802 per ton (RSMeans 2016). The installed cost of a two-ton GSHP is $3483 (RSMeans 2016). This gives a total system cost of $15,487 for a GSHP with a VBGHE. For a GSHP with a UTB which was installed with casing, the GHE cost is relatively expensive. In this case, the system cost of a GSHP with two tank UTB is estimated at $16,968. The system cost of a GSHP with a single tank UTB is estimated at $14,114.

For a GSHP with a UTB which was installed without casing, the GHE cost is relatively inexpensive. In this case, the system cost of a GSHP with two tank UTB is estimated at $13,120. The system cost of a GSHP with a single tank UTB in this case is estimated at $12,032.

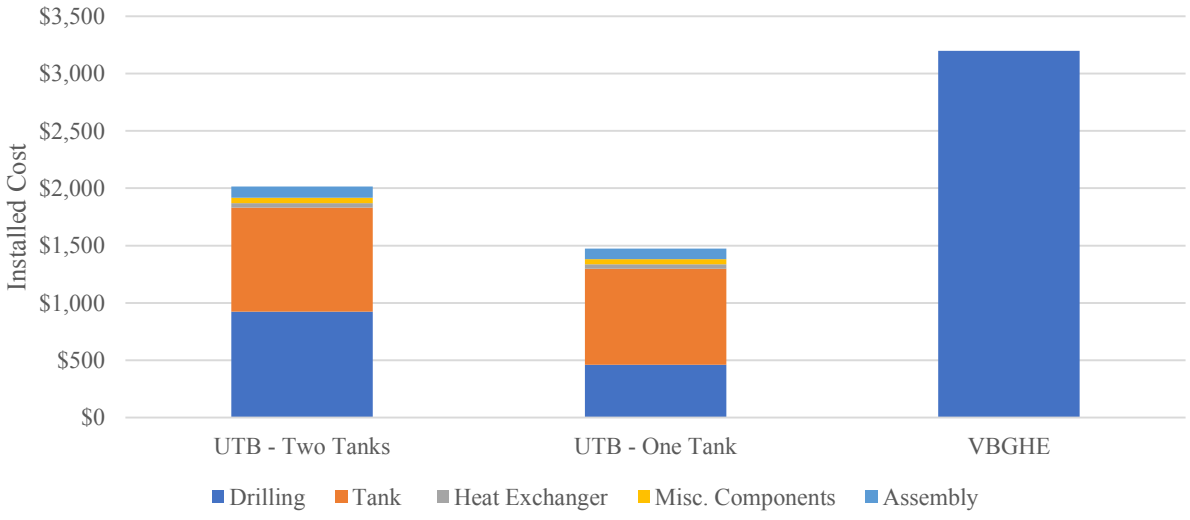

Figure 34. Cost comparison for UTBs installed using auger drilling without casing.

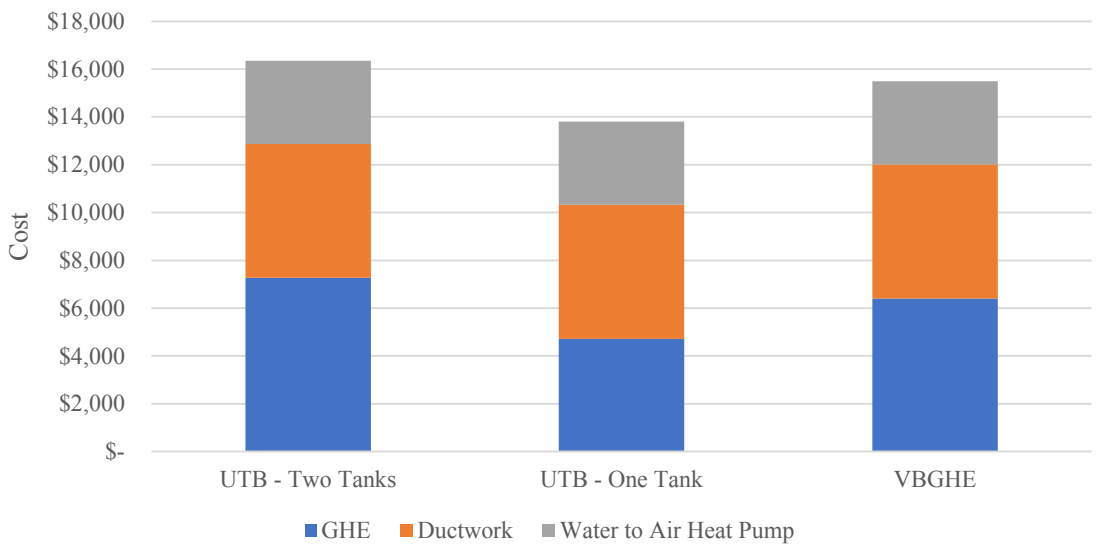

Figure 35. System cost comparison for GSHP systems with ground heat exchangers installed using auger drilling with casing.

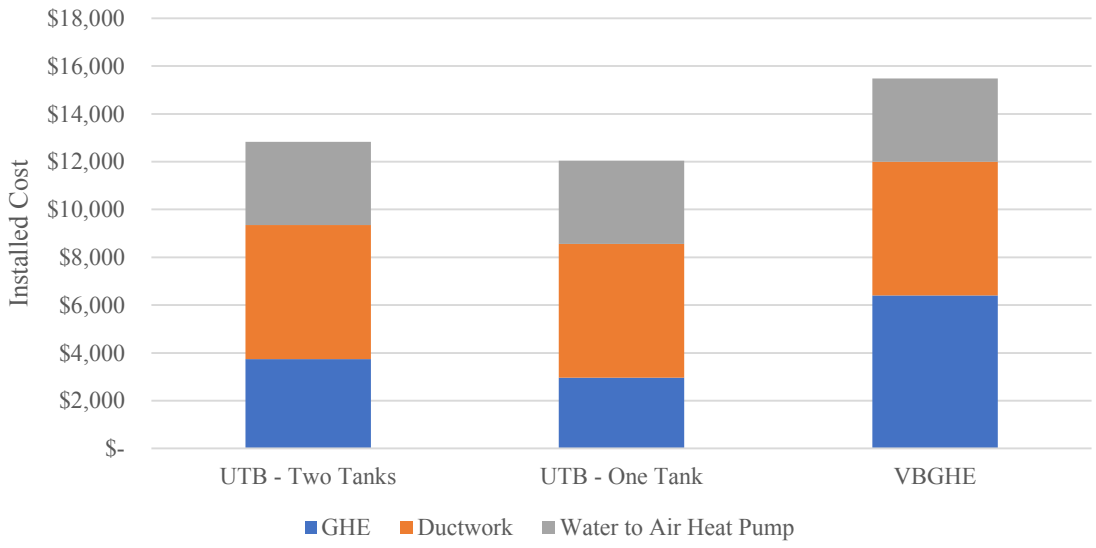

Figure 36. System cost comparison for GSHP systems with ground heat exchangers installed using auger drilling without casing.

4.4 Conventional HVAC Cost Estimate

A model for the price of a baseline residential HVAC system was established by (Liu et al. 2019). using data from RSMeans (2016). This model includes the installed cost of the space cooling and space heating equipment, as well as ductwork. Based on a system rating of 2 tons of space cooling capacity, the space cooling equipment is priced at $4305. A natural gas system is used for space heating in this model. For a space heating capacity of 80 MBH, the equipment cost is priced at $1080. The ductwork is again priced at $2802 per ton, for a total cost of $5604. This gives a total system cost of $10,989 for the conventional HVAC system.

The cost premium for each ground heat exchanger can be calculated from this baseline. The cost premium is a critical factor in the market penetration of an energy saving technology. By reducing the cost premium, the energy cost savings requirement for market feasibility is also reduced. Figure 38 shows the cost premium for the UTB and VBGHE over the conventional HVAC. The UTB with casing has a lower cost premium than the VBGHE if a single tank configuration is used, but a higher premium if two tanks are needed. However, if drilling without casing the cost premium is significantly lower for either UTB configuration. This represents a significant improvement over the conventional technology. In fact, the cost premium is reduced by 53% for the single tank and 77% for the two tank UTB.

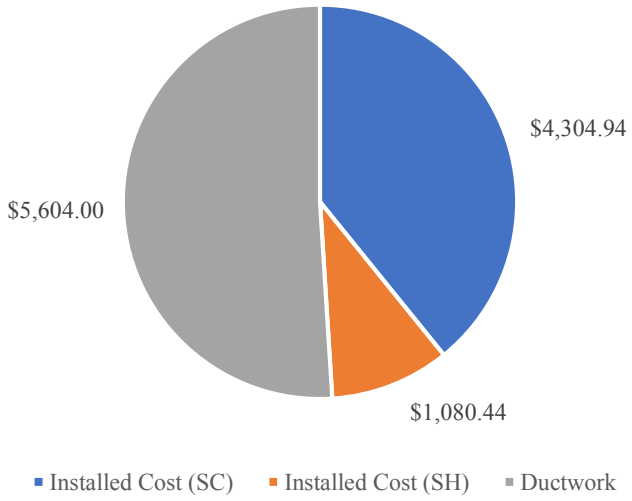

Figure 37. Cost breakdown for a conventional HVAC system.

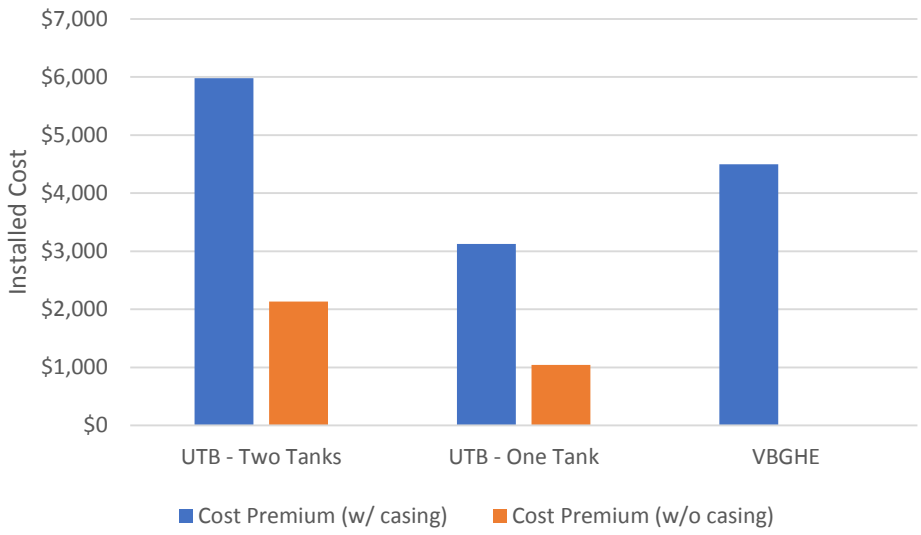

Figure 38. System cost premium for GSHP systems compared with conventional HVAC.

4.5 Case Study – Cost Analysis

A case study simulation of a small residential home with a cooling capacity of 2 tons was conducted using eQuest to evaluate the cost savings potential of the UTB. Knoxville weather data was used in the simulation, and the HVAC equipment performance data is presented in Table 9 below.

The two modes of energy consumption for a conventional HVAC system are electricity consumption and natural gas consumption. An air conditioning air-to-air heat pump unit is used for cooling mode and consumes electricity with a COP of 3.78 W/W in this case. A natural gas furnace is used for heating mode and consumes natural gas with an efficiency of 81%. The monthly energy consumption of the conventional HVAC is presented in Figure 39. As can be seen from this graph, the electricity consumption peaks during the summer when cooling loads are highest, and the natural gas consumption peaks during the winter when heating loads are highest. Comparing this to the ground source heat pump with a VBGHE, presented in Figure 40, we can see that the natural gas consumption is replaced with year-round electricity consumption from the heat pump. The high efficiency of the heat pump means that less energy is used throughout the year. This, along with the removal of the natural gas consumption results in energy cost savings for the GSHP system. Accounting for all sources of electricity consumption in a residential household, the total energy consumption can be reduced by 13% for an annual energy cost savings of $245.5 for this case. It is important to note that this is a particularly mild climate. In more severe climates the savings may be more significant.

Table 9. Simulation Data for GSHP and Conventional HVAC (baseline)

Residence Square Footage	1199 sq. ft.
GSHP cooling COP	5.88 W/W
GSHP heating COP	4.5 W/W
Baseline AC COP	3.78 W/W
Baseline Furnace efficiency	81%

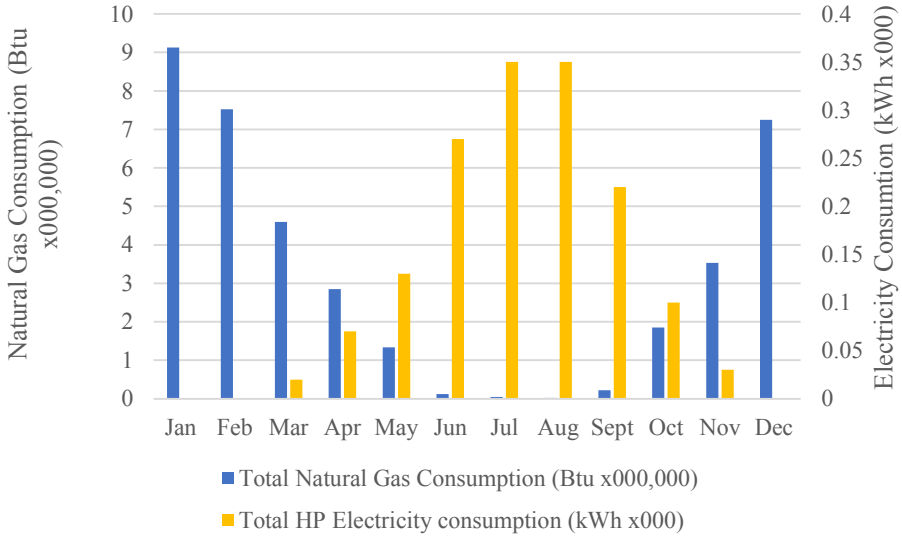

Figure 39. Energy consumption by month for conventional 2-ton HVAC in Knoxville, TN.

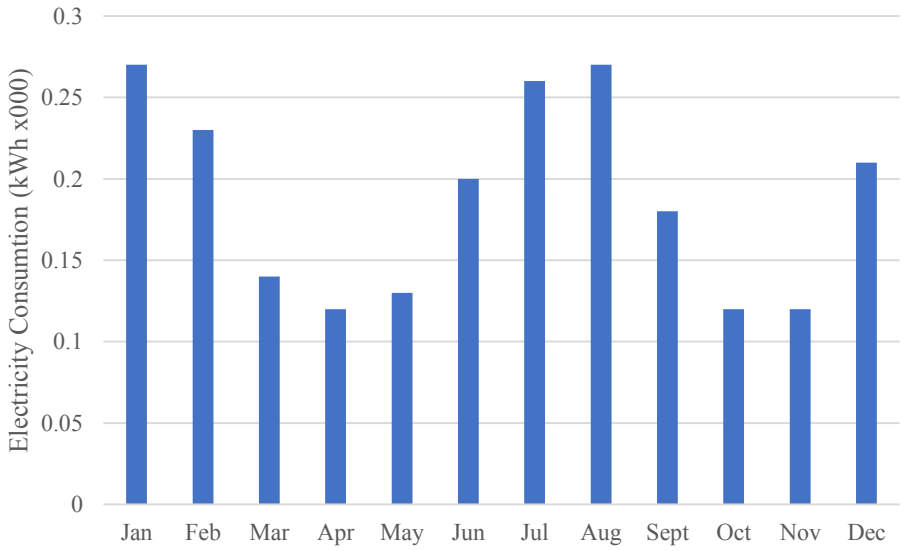

Figure 40. Energy consumption by month for conventional 2-ton GSHP in Knoxville, TN.

The energy cost savings of the GSHP with a UTB GHE are estimated by comparing the simulated results of a GSHP with UTB with that of a VBGHE for the same thermal loads. The energy consumption is determined for each using the simplified heat pump model to determine the heat pump performance based on the heat exchanger outlet temperature. The percentage difference in the annual energy consumption is used as a modifier on the above annual energy consumption results of the eQuest simulation to give a fair comparison between the systems. The simulated UTB configurations consisted of a single UTB with 42" diameter and 20' depth with no PCM, and a UTB with two 30" tanks and 20' depth with no PCM. The single UTB tank had an annual energy consumption which was 12% higher than the VBGHE, and the UTB with two tanks had an annual energy consumption which was approximately the same as the VBGHE.

The payback period (in years) is calculated by dividing the cost premium by the annual cost savings:

$$payback\ period = \frac{cost\ premium}{annual\ energy\ cost\ savings}$$

Based on the cost premium of each configuration and the annual energy savings, the payback period is presented in Figure 41. The conventional VBGHE has a payback period of approximately 18 years in this case. This is higher than average due to the mild thermal loads in the Knoxville climate, which reduce the potential for energy savings. For the UTB, the payback period is higher with two tanks with casing and lower for the single tank case with casing. However, without casing, the payback period is significantly reduced over the VBGHE. With two tanks it is reduced to less than 9 years and with a single tank it is reduced to less than 5 years. This reaches a significant benchmark for the market penetration of a renewable technology, as it is widely considered that a payback period of 5 years is required for mass adoption of an energy saving technology.

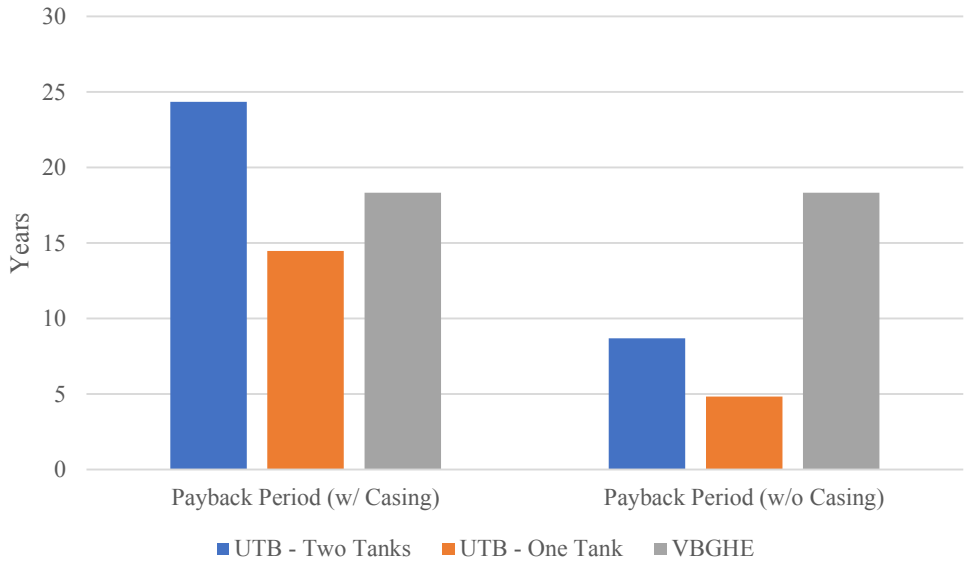

Figure 41. Payback period for various GSHP GHE configurations for a 2-ton GSHP system in Knoxville, TN.

CHAPTER 5: Conclusions and Recommendations for Future Work

5.1 Conclusions: Modeling

This paper introduces a one-dimensional model of a novel ground heat exchanger, the Underground Thermal Battery (UTB). This model was validated against the prediction of a more detailed 3-D model of the UTB. The validated 1-D model was used to investigate the performance of the UTB over a year-long operation. Leaving fluid temperature of the UTB under the thermal loads of a residential GSHP system during a year was predicted with the 1-D model and it was compared the leaving fluid temperature of a conventional VBGHE. A parametric study was also conducted to investigate the performance of various UTB configurations and operating conditions. In addition, the impacts of varying soil temperature on the predicted performance of the UTB was investigated. The impacts of integrating the UTB with a pre-existing irrigation system was also investigated through simulations using the 1-D model. The results of this study indicate that:

- Over a year-long operation, a UTB with two 22 ft. deep tanks can achieve the similar performance to a conventional 200 ft. deep VBGHE over most climates and ground thermal conductivities.
- Surface area is the most important factor in determining the performance of the UTB for a given set of operating conditions. In this study, the performance of the VBGHE could be approximately matched with a UTB that has the same surface area.
- The PCM does not cycle frequently as expected due to the thermal buildup in the tank which prevents the UTB temperature from returning below the phase change temperature of the PCM. Active cooling with nature resources, such as a dry cooler or a radiative cooling with the sky, should be investigated to enable cyclic operation of the PCM and allow the UTB to reach its maximum cost reduction or energy saving potential.
- Integrating the UTB with the lawn irrigation system of the residence can partially recharge the UTB and increase the cycling frequency of the PCM. It thus improves the UTB performance. It also may allow for the use of a single-tank UTB, which can further reduce the cost.

The UTB can be installed at a lower cost than the conventional VBGHE due to the shallow hole which requires less expensive equipment to drill. This could make GSHP systems more economically viable and will enable a wider adoption of the GSHP technology, thereby reducing energy consumption and carbon emissions.

The UTB has been shown to be an effective alternative of conventional vertical bore ground heat exchanger. However, the value of the UTB could be increase if its large thermal energy storage capacity can be fully utilized. Further study into combining the UTB with other renewable energy sources is necessary. Given the capacity of actively storing and releasing thermal energy on a daily basis, UTB has significant potential to help reshape the electric demand of buildings and thus help improve the grid stability in the era with increased penetration of intermittent renewable energy supply.

5.2 Conclusions: Cost Analysis

The cost analysis section introduces a cost model of the necessary components to construct a UTB, as well as a model for the system level components including the GSHP and ductwork. The model was used to estimate the cost of various configurations of conventional HVAC and GSHP systems, including various ground heat exchangers. A case study was conducted in which eQuest software was used to simulate the annual performance of the systems to determine the annual cost savings potential of each design. This cost savings was combined with the cost premium over the conventional HVAC to determine the payback period for each GSHP configuration. The results of this analysis indicate:

- Over a year-long operation in Knoxville, the GSHP with VBGHE has an annual energy cost savings of 13% over a conventional HVAC, with a monetary savings of $298. The UTB with two tanks can approximately match this performance in this case study.
- The UTB with a single tank has a lower cost premium than the VBGHE, but with an increase in energy consumption of approximately 13% in this case. This suggests some cost-benefit analysis is necessary for each case.
- The use of casing has a significant impact on the cost premium and thereby the payback period of the UTB. With no casing, a single tank UTB can have a payback period of just 5 years for this case study. A UTB with two tanks also sees a significant reduction in payback period, at just 8 years.

The UTB configurations have the potential to be installed at a lower cost than the conventional VBGHE due to the shallow hole which requires less expensive equipment to drill. This could make GSHP systems more economically viable and enable a wider adoption of GSHP technology.

5.3 Future Work

This work represents an initial investigation into the feasibility of the UTB as an effective ground heat exchanger for GSHP technology. Further study is necessary to refine the evaluation of this technology and develop a better understanding of its capabilities. Several key areas of study are necessary:

- Active cooling with natural resources, such as a dry cooler or radiative cooling with the sky, should be investigated to enable cyclic operation of the PCM and allow the UTB to reach its maximum cost reduction or energy saving potential.
- The implementation of a 2-D soil heat transfer model with surface heat flux is necessary to more accurately predict the effects of ground temperature fluctuations on UTB performance.
- A more comprehensive cost analysis is needed to gain a better understanding of the cost saving potential of the UTB due to low-cost auger drilling.

The UTB has been shown to have significant potential as an energy-saving technology. However, for this potential to be realized it must be studied further to better understand its capabilities and to promote its commercialization.

REFERENCES

L. D&R International, *2011 Buildings Energy Data Book*. 2011.

Z. Liu, W. Xu, X. Zhai, C. Qian, and X. Chen, "Feasability and performance study of the hybrid ground-source heat pump system for one office building in Chinese heating dominated areas," *Renew. Energy*, vol. 101, pp. 1131-1140, 2017.

Liu, X., Y. Polsky, D. Qian, J. Mcdonald. 2019. "An Analysis on Cost Reduction Potential of Vertical Bore Ground Heat Exchangers Used for Ground Source Heat Pump Systems". PROCEEDINGS, 43rd Workshop on Geothermal Reservoir Engineering, Stanford University, Stanford, California, February 11-13, 2019

Palm, B., and M. Ignatowicz. 2016. "Adsorption Corrosion Inhibitors, Green Corrosion Inhibitors and Alternative Secondary Fluids for Indirect Systems." Retrieved 7/15/2016, from http://effsysexpand.se/p03-adsorberande-korrosionsinhibitorer/.

ClimateMaster, 2016. *Tranquility 30 Digital (TE) Series Submittal Data – Models TED/H/V 026–072–HFC-410A*. Available at *http://www.climatemaster.com/downloads/lc991-climatemaster-commercial-tranquility-30-digital-two-stage-te-series-water-source-heat-pump-submittal-set.pdf*

NYSERDA, 2017. *Renewable Heating and Cooling Policy Framework*.

Lund, J. W. 2001 "Geothermal heat pumps-An overview." *Geo-Heat Center Quarterly Bulletin 22(1):1-2*.

Bertermann, David, et al. *European Project 'Cheap-GSHPs': Installation and Monitoring of Newly Designed Helicoidal Ground Source Heat Exchanger on the German Test Site*. SpringerLink, Springer, Dordrecht, 27 Deb. 2018, link.springer.com/article/10.1007/s12665-018-7343-4.

Y. Rabin and E. Korin, "Incorporation of phase-change materials into a ground thermal energy storage system: Theoretical study," *J. Energy Resour. Technol. Asme*, vol. 118, no. 3 pp. 237-241, 1996

H. Benli, A. D.-E. and Buildings, and U. 2009, "Benli, Durmus – 2009 – Evaluation of ground-source heat pump combined latent heat storage system performance in greenhouse heating(2).pdf," *Elsevier*.

Bottarelli et al. Numerical analysis of a novel ground heat exchanger coupled with phase change materials. *Applied Thermal Engineering* 88 (2015) 369-375.

Bonamente et al. A PCM thermal storage for ground-source heat pumps: simulating the system performance via CFD approach. *Energy Procedia* 101 (2016) 1079-1086.

Sachs, H. 2002. *Geology and drilling methods for ground-source heat pump installations*. ASHRAE, Atlanta.

GEOteCH. 2016. *GEOthermal Technology for economic Cooling and Heating*.

C.L. Zhang, W. He, S.L. Wang, W.J. Guan, J.Y. Jia, *Discussion of operating modes of GSHP combined with ice storage systems*, HV&AC 38 (2) (2008) 122-124.

X.J. Dong, B. Gu, S.Q. Ye, Y.L. Chen, et al., Operation simulation of ground-source heat pump combined with ice thermal storage, HV&AC 40 (6) (2010) 45-48.

Z. Melikyan, V. Melikyan, Ice storage geothermal heat pump, in: 20th Wrold Energy Engineering Congress (WEEC), Atlanta, GA, Nov 19-21, 1997.

B. Stojanovic, J. Akander, Build-up and long-term performance test of a full-scale solar-assisted heat pump system for residential heating in Nordic climatic conditions, Appl. Therm. Eng. 30 (2-3) (2010) 188-195.

Cordts, D. 2011. "The GeoColumn™ Geothermal Heat Pump Company." *Geothermal Energy Workshop*. April 13, 2011.

Tiedje, E., and P. Guo. 2014. "Thermal Conductivity of Bentonite Grout Containing Graphite or Chopped Carbon Fibers." *Journal of Materials in Civil Engineering* 26(7), https://doi.org/10.1061/(ASCE)MT.1943-5533.0000977.

P. Eslami-nejad, M. Bernier, Coupling of geothermal heat pumps with thermal solar collectors using double U-tube boreholes with two independent circuits, Appl. Therm. Eng 31 (14-15) (2011) 3066-3077.

H.J. Wang, C.Y. Qi, Performance study of underground thermal storage in a solar-ground coupled heat pump system for residential buildings, Energy Build. 40 (7) (2008) (1278-1286)

H.J. Wang, C.Y. Qi, A case study of underground thermal storage in a solaer-groudn coupled heat pump system for residential buildings, Renew. Energy 34 (1) (2009) 307-314.

E. Kjellsson, G. Hellstrom, B. Perers, Optimization of systems with the com-bination of ground-source heat pump and solar collectors in dwellings, Energy 35 (6) (2010).

Y.S. Qi, Y.L. Yue, T.Y. Liu, D.L. Yuan, Application analysis of combined ground-sourcce heat pump and water energy storage systems HV&AC 40 (5) (2010) 94-97.

Liu X., et al. 2018. *GeoVision Analysis: Thermal Applications Task Force Report – Geothermal Heat Pumps*. ORNL/TM-2017/502. Oak Ridge, Tennessee: Oak Ridge National Laboratory.

Gonthier, S. 2012. "GEOPERFORMX Thermally Enhanced Pipe for Geothermal Applications." 2012 *Annual Conference of International Ground Source Heat Pump Association*. October 4th, 2012.

Water Research Foundation. (2016, April). *Residential End Uses of Water, Version 2*. Retrieved from Water Research Foundation: http://www.waterrf.org/PublicReportLibrary/4309A.pdf

Muhieddine, M., Canot, É, & March, R. (2009). Various Approaches for Solving Problems in Heat Conduction with Phase Change. *International Journal on Finite Volumes*,*6*(1).

D. Qi, L. Pu, F. Sun, and Y. Li, "Numerical investigation on thermal performance of ground heat exchangers using phase change materials as grout for ground source heat pump system," *Elsevier*, vol. 106, pp. 1023–1032, 2016.

NREL (2015). Overgeneration from Solar Energy in California: A Field Guide to the Duck Chart. https://www.nrel.gov/docs/fy16osti/65023.pdf

Agrisupply, (2019). Retrieved from www.agrisupply.com.

F. W. Webb (2019). Retrieved from www.fwwebb.com

McMaster Carr (2019). Retrieved from www.mcmaster.com.

VITA

Joseph Warner was born in Florence, SC, to the parents of Ronald and Sarah Warner. He attended high school at Middle Tennessee Christian School where he was the valedictorian of his class. After graduation, he enrolled in the University of Tennessee, Knoxville where he began his study of Mechanical Engineering. During this period, he completed multiple internships at the Oak Ridge National Laboratory and furthered his passion for engineering. In May 2017, he obtained a Bachelor of Science degree in Mechanical Engineering, with the honor of Magna Cum Laude. He accepted a graduate research position at the University of Tennessee, Knoxville, and began working on renewable energy research at the Oak Ridge National Laboratory. Joseph graduated with a Master of Science degree in Mechanical Engineering, with a concentration in thermal fluid mechanics, in May 2019.